AD-A049 153 NAVAL RESEARCH LAB WASHINGTON D C F/G 11/6
EFFECT OF HOLD TIME AND THERMAL AGING ON ELEVATED TEMPERATURE F--ETC(U)
OCT 77 D J MICHEL, H H SMITH E(49-5)-2110
UNCLASSIFIED NRL-MR-3627 SBIE-AD-E000 058 NL

1 OF 1
AD
A049153

END
DATE
FILMED
3 78
DDC

12

NRL Memorandum Report 3627

Effect of Hold Time and Thermal Aging on Elevated Temperature Fatigue Crack Propagation in Austenitic Stainless Steels

D. J. MICHEL and H. H. SMITH

Thermostructural Materials Branch
Engineering Materials Division

October 1977

NAVAL RESEARCH LABORATORY
Washington, D.C.

SECURITY CLASSIFICATION OF THIS PAGE (When Data Entered)

REPORT DOCUMENTATION PAGE		READ INSTRUCTIONS BEFORE COMPLETING FORM
1. REPORT NUMBER NRL Memorandum Report 3627	2. GOVT ACCESSION NO.	3. RECIPIENT'S CATALOG NUMBER 9
4. TITLE (and Subtitle) 6 EFFECT OF HOLD TIME AND THERMAL AGING ON ELEVATED TEMPERATURE FATIGUE CRACK PROPAGATION IN AUSTENITIC STAINLESS STEELS.		5. TYPE OF REPORT & PERIOD COVERED Interim ~~topical~~ report, on a continuing problem.
		6. PERFORMING ORG. REPORT NUMBER
7. AUTHOR(s) 10 D.J. Michel ~~and~~ H.H. Smith		8. CONTRACT OR GRANT NUMBER(s) 15 E(49-5)-2110
9. PERFORMING ORGANIZATION NAME AND ADDRESS Naval Research Laboratory Washington, D.C. 20375		10. PROGRAM ELEMENT, PROJECT, TASK AREA & WORK UNIT NUMBERS NRL Problems M01-14 & M01-27 Project E(49-5)-2110 & RR022-11-41-5426
11. CONTROLLING OFFICE NAME AND ADDRESS Office of Naval Research; and Energy Research and Development Administration Washington, D.C. 20545		12. REPORT DATE 11 October 1977
		13. NUMBER OF PAGES 45
14. MONITORING AGENCY NAME & ADDRESS(if different from Controlling Office) 12 46p.		15. SECURITY CLASS. (of this report) UNCLASSIFIED
		15a. DECLASSIFICATION/DOWNGRADING SCHEDULE

16. DISTRIBUTION STATEMENT (of this Report)

Approved for public release; distribution unlimited.

14 NRL-MR-3627

DDC
RECEIVED
JAN 31 1978
B

17. DISTRIBUTION STATEMENT (of the abstract entered in Block 20, if different from Report)

16 RRØ2211 17 RRØ221141

18. SUPPLEMENTARY NOTES

18 SBIE 19 AD-E000 058

19. KEY WORDS (Continue on reverse side if necessary and identify by block number)

Crack propagation	Fatigue	Mechanical properties
Creep-fatigue interaction	Flaw growth	Precipitate formation
Elevated temperatures	Grain boundary sliding	
Environment effects	Hold time	

20. ABSTRACT (Continue on reverse side if necessary and identify by block number)

The effects of combined cyclic and static loading on fatigue crack propagation in thermally aged and unaged Types 304, 316, 321, and 348 stainless steels were investigated at 427 and 593°C. The Types 304 and 316 steels were evaluated in both the solution annealed and cold worked conditions. The results show that aging and hold time produce no significant effect on crack propagation rate at 427°C. At 593°C, the effects of aging on crack propagation performance were most significant for the Type 316 steel and were related to thermomechanical history. Thermal aging decreased the crack propagation rate in solution annealed Type 316 (Continued)

DD FORM 1 JAN 73 1473 EDITION OF 1 NOV 65 IS OBSOLETE
S/N 0102-014-6601

i

SECURITY CLASSIFICATION OF THIS PAGE (When Data Entered)

251 950 4B

20. ABSTRACT (Continued).

steel at 539°C and increased the propagation rate in cold worked material. The effect of hold time at 593°C was to increase crack propagation rate with increased hold period in Type 316 steel. In the cold worked Type 316 steel, thermal aging reduced the magnitude of the hold time effect. SEM examination of the fracture surfaces of both solution annealed and cold worked Type 316 specimens tested at 593°C revealed a transition from transgranular to intergranular failure mode with increasing hold time in the unaged condition. After thermal aging, the failure mode was transgranular for all hold times. TEM study of the aged and unaged microstructures indicated the presence of profuse grain boundary precipitates identified as $M_{23}C_6$. Consideration was given to influence of both environmental effects and the intergranular precipitates on the transition in failure mode. Based on the experimental evidence, it was concluded that intergranular precipitates provided the primary influence on the crack propagation response by the suppression of grain boundary sliding during hold periods at 593°C thereby delaying the transition in failure mode from transgranular to intergranular.

CONTENTS

EFFECT OF HOLD TIME AND THERMAL AGING ON ELEVATED TEMPERATURE FATIGUE CRACK PROPAGATION IN AUSTENITIC STAINLESS STEELS

INTRODUCTION

The service conditions of advanced nuclear systems are expected to impose the combined effects of static and cyclic loading on the structural components at sustained elevated temperatures. Under these conditions, the propagation of cracks which may originate from flaws or pre-existing small cracks in the components will be influenced by the thermal stability of the structural material. Since it is known that the sustained elevated temperature exposure of many materials can produce the precipitation of various intermetallic phases, consideration must be given to the investigation of the effects of thermal stability on the creep-fatigue crack propagation behavior of structural materials.

Relatively few investigations of creep-fatigue interaction effects on crack propagation at elevated temperatures have been reported. Recent work by Michel et al. (1,2,3) has shown that the inclusion of tensile hold times of 0.1 and 1 minute have no significant effect on crack growth rate in solution annealed and 20 percent cold worked Type 316 stainless steel at 427°C (800°F). However, at 593°C (1100°F), the effect of tensile hold time was found to significantly increase crack propagation rate (da/dN) in 20 percent cold worked Type 316 stainless steel but not in solution annealed material. From these results it was concluded that recovery processes rather than environmental effects contributed to the increased crack growth rates observed in the cold worked material at 593°C.

Other previous work was briefly reviewed by Michel et al. (1,2,3) and additional recent results have been presented by Shahinian (4). Work by Nicholson (5) on creep crack propagation in solution annealed Type 316 stainless steel at temperatures in the range from 600 to 850°C (1200 to 1562°F) has shown that crack growth rates, da/dt, under static loading are controlled by displacement rates at the crack tip and by the ligament strain. Wareing (6) has concluded that the reduction in fatigue life for hold periods at maximum tensile

Note: Manuscript submitted September 29, 1977.

strain are the result of the interaction between creep damage during stress relaxation and the propagating crack. Other work by Shahinian (7) has shown that creep crack propagation rate in cold worked Types 304 and 316 stainless steel was lower than in fatigue at 482°C and at $\Delta K < 25\ MPa\sqrt{m}$ at 593°C.

Considerable research has shown that the long term exposure of austenitic stainless steels to elevated temperatures is responsible for the precipitation of intermetallic phases (8,9) which can influence the mechanical properties (10-13) of the steels. Few studies have considered the effects of thermal aging on fatigue crack propagation in the austenitic stainless steels (3,14). Michel et al.(3) have shown that 0.1 and 1.0 minute hold times and/or prior thermal aging did not influence the fatigue crack propagation behavior of Type 316 steel at 427°C. At 593°C, thermal aging was found to reduce the magnitude of the increase in crack propagation rate produced by increased hold times in both steels. In the study by James (14), it was found that thermal aging produced lower crack propagation rates relative to unaged material during continuous cycling at 538 and 650°C (1000 and 1200°F). However, one hold time test conducted by James (14) indicated little effect of thermal aging on crack propagation rate in Type 304 steel.

The purpose of this report is to summarize the results obtained by Michel et al. (1,2,3) on the effects of hold time and thermal aging on elevated temperature fatigue crack propagation in Types 304 and 316 stainless steel. New results obtained for Types 321 and 348 stainless steel also are presented. The results are compared on the basis of the combined effects of cyclic loading with periods of static tensile loading (hold times) of 0, 0.1, and 1.0 minutes and prior thermal aging for 5000 hours at 593°C. The influence of thermomechanical history, environment, and microstructure on crack propagation and failure mode are discussed.

EXPERIMENTAL PROCEDURE

The chemical compositions of Types 304, 316, 321, and 348 stainless steel plate used in the study are given in Table 1. All materials received similar processing histories. The cold worked material condition was produced by rolling at ambient temperature to achieve the desired reduction in thickness. Optical micrographs of the Types 316 and 304 starting materials are shown in Fig. 1. Single-edge-notched cantilever specimens, containing side grooves to a depth of 5 percent of the specimen thickness, were prepared to the specifications shown in Fig.2. The specimen orientation was such that the plane of crack growth was perpendicular to the rolling direction of the plate material.

TABLE 1

Chemical Composition, Weight Percent

Steel (Heat Number)	C	Mn	P	S	Si	Cr	Ni	Other
304 SS (Heat A) (Carlson K44086-1B)	0.048	1.48	0.025	0.015	0.52	18.57	9.45	
304 SS (Heat B) (U.S.Steel 9T2796)	0.048	1.18	0.032	0.016	0.48	18.56	9.80	Mo-0.31; Cu-0.22
316 SS (Allegheny Ludlum 65808)	0.060	1.72	0.012	0.007	0.40	17.30	13.30	Mo-2.33; Cu-0.65; Co-0.30; Al-0.012; Ti-0.003; B-0.0005
321 SS (Carlson 600251-2)	0.031	1.38	0.013	0.010	0.66	17.71	10.00	Ti-0.27
348 SS (Carpenter 89107)	0.062	1.82	0.006	0.007	0.52	18.64	9.86	Mo-0.06; Cu-0.02; Co-0.01

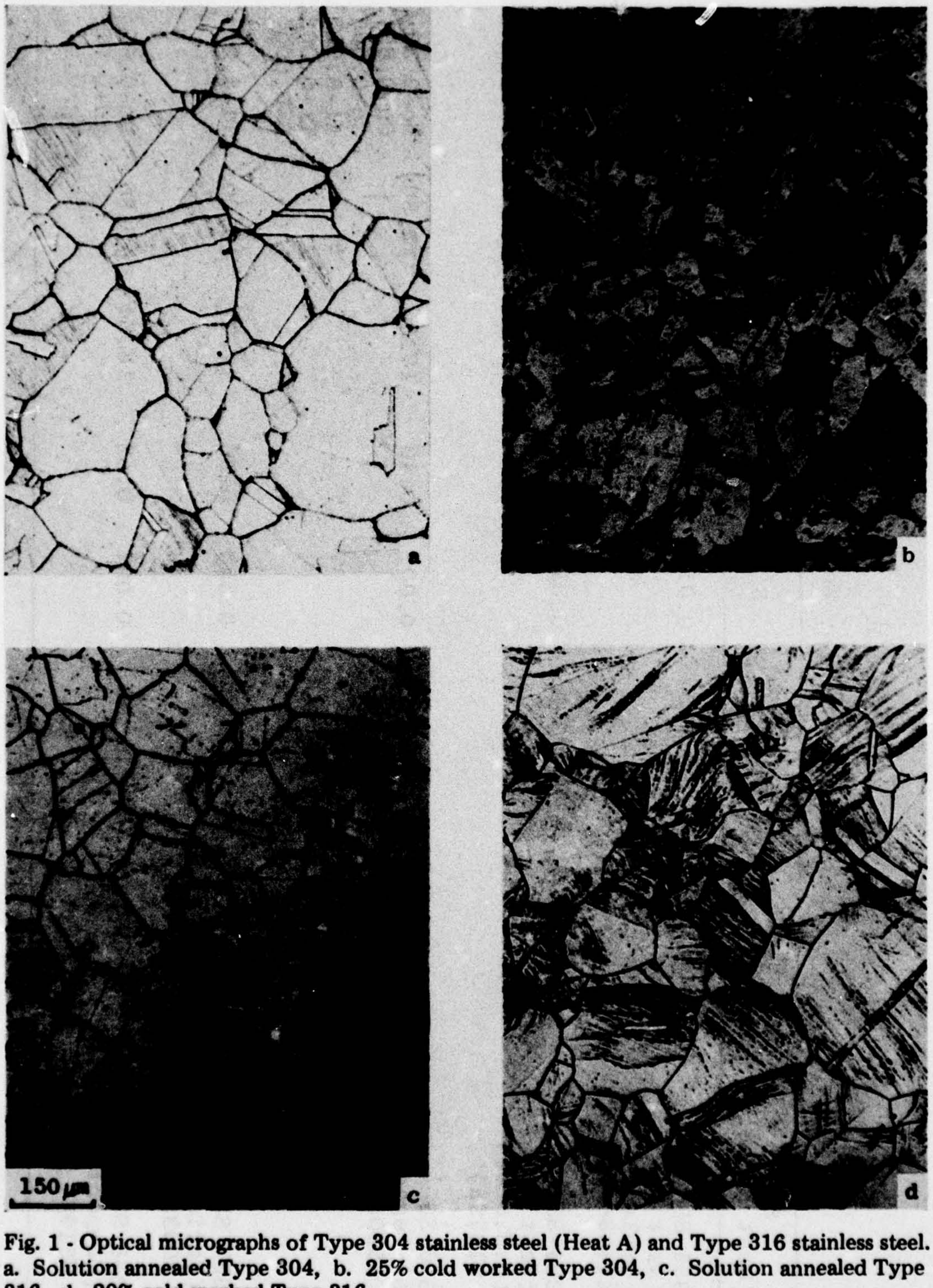

Fig. 1 - Optical micrographs of Type 304 stainless steel (Heat A) and Type 316 stainless steel. a. Solution annealed Type 304, b. 25% cold worked Type 304, c. Solution annealed Type 316, d. 20% cold worked Type 316.

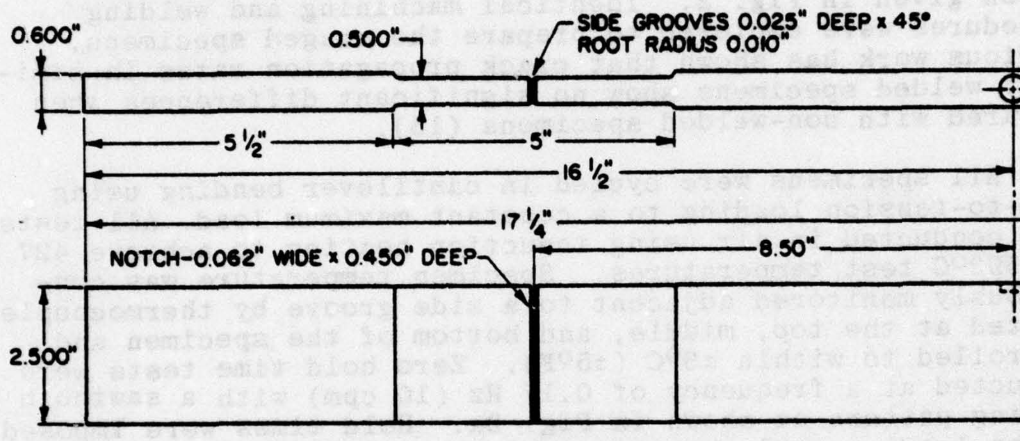

Fig. 2 - Specifications of test specimens (1 inch = 25.4 mm).

To evaluate the effects of sustained elevated temperature exposure, specimen center sections 55.9 x 63.5 mm (2.2 x 2.5 in.) were thermally aged for 5000 hours at 593°C in electric muffle furnaces in air. These aging conditions were chosen on the basis that 593°C represents the approximate upper service limit of the austenitic stainless steels and that, after 5000 hours, precipitation of the $M_{23}C_6$ carbide phase is essentially complete according to recent phase stability studies (8,9). After machining, end tabs were welded to the center sections to produce the final specimen configuration given in Fig. 2. Identical machining and welding procedures were employed to prepare the unaged specimens. Previous work has shown that crack propagation rates in similarly welded specimens show no significant differences when compared with non-welded specimens (15).

All specimens were cycled in cantilever bending using zero-to-tension loading to a constant maximum load. All tests were conducted in air using induction heating to achieve 427 and 593°C test temperatures. Specimen temperature was continuously monitored adjacent to a side groove by thermocouples located at the top, middle, and bottom of the specimen and controlled to within ±3°C (±5°F). Zero hold time tests were conducted at a frequency of 0.17 Hz (10 cpm) with a sawtooth loading pattern as shown in Fig. 3a. Hold times were imposed on the loading cycle by maintaining the maximum tensile load constant for 0.1 or 1.0 minutes as illustrated in Fig. 3b.

Crack length was measured during testing at the root surface of a side groove using a traveling microscope. The tests were terminated when the sum of the crack length plus edge notch depth was approximately 40.6 mm (1.6 in.) since gross plastic deformation was evident at the crack tip, particularly at the 593°C test temperature.

Crack growth rates, da/dN, were determined from the slopes of crack length versus number of cycles plots and correlated with the crack-tip stress intensity factor range, ΔK, computed according to the expression for pure bending given by Gross and Srawley (16):

$$K = \frac{6PL}{(B \cdot B_N)^{1/2} \, W^{3/2}} \cdot Y, \qquad (1)$$

where, $Y = 1.99\,(a/W)^{1/2} - 2.47\,(a/W)^{3/2} + 12.97\,(a/W)^{5/2} - 23.17\,(a/W)^{7/2} + 24.80\,(a/W)^{9/2}$,

and P is the maximum load, L is the distance from crack plane to point of load application, a is the total length of crack

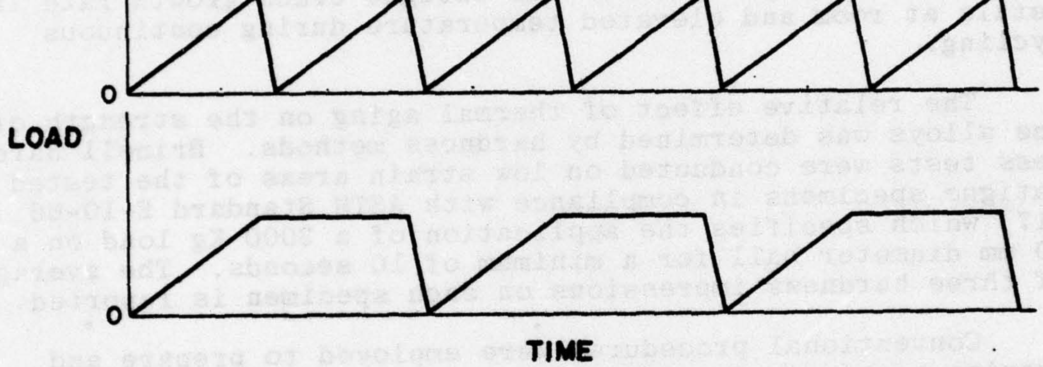

Fig. 3 - Wave forms used for fatigue tests. a. 0.17 Hz (10 cpm), zero hold time, b. 0.17 Hz (10 cpm) with 0.1 or 1 minute hold times.

and notch, W is the specimen width, B is the specimen thickness, and B_N is the net specimen thickness at the side grooves. Corrections for crack tip plasticity were not applied to the data. All calculations were conducted using a programmable digital calculator according to the procedures outlined in Appendix A.

The experimental data were analyzed on the basis of the power law relationship:

$$da/dN = C(\Delta K)^m, \qquad (2)$$

where C and m are constants dependent on the material and environmental factors, respectively. It is well known that this relationship describes the fatigue crack growth rate in metals at room and elevated temperature during continuous cycling.

The relative effect of thermal aging on the strength of the alloys was determined by hardness methods. Brinell hardness tests were conducted on low strain areas of the tested fatigue specimens in compliance with ASTM Standard E-10-66 (17) which specifies the application of a 3000 Kg load on a 10 mm diameter ball for a minimum of 10 seconds. The average of three hardness impressions on each specimen is reported.

Conventional procedures were employed to prepare and examine specimens for transmission and scanning electron microscopy (TEM and SEM). Thin foils for transmission study were prepared according to previously reported techniques (18) from specimen sections located outside of the plastic zone. The foils were examined and photographed using a JEM-200A transmission microscope operated at 200 kV. Selected area diffraction and dark field imaging procedures were used to identify the precipitates. For the fractographic examinations, the fracture surface and approximately 3 mm of adjoining material were sectioned from the test specimen and treated with an inhibited 6N HCl acid solution to remove the bulk oxide scale. These surfaces were then examined using a Coates and Welter, Cwikscan 106A SEM operated at an accelerating voltage of 900 volts.

RESULTS

Crack Propagation

The effects of hold time and prior thermal aging on fatigue crack propagation in solution annealed Types 316 and 304 at 427°C are shown in Figs. 4 and 5. Experimental results at 593°C for annealed Types 316, 304, 321, and 348 stainless steel are shown in Figs. 6 through 11. Figures 12 through 14 depict the effects of hold time and thermal aging on fatigue

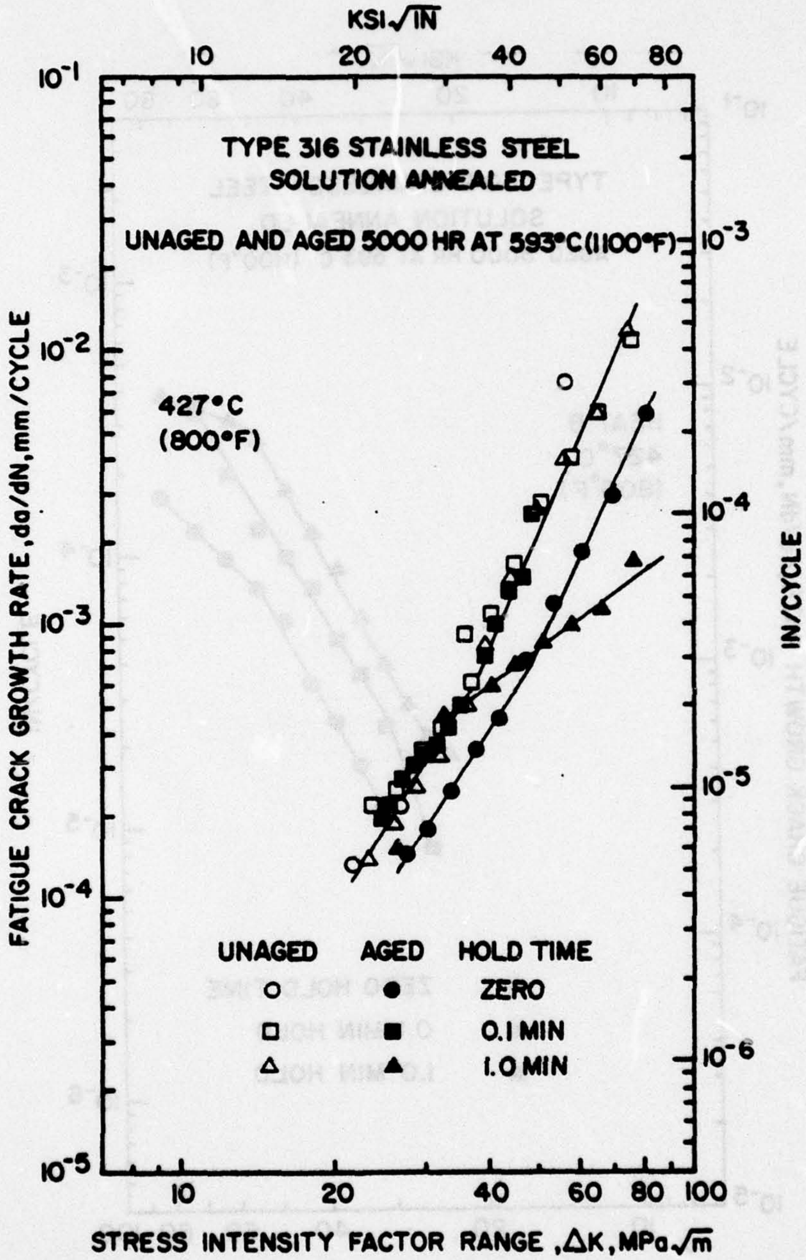

Fig. 4 - Effect of thermal aging and hold time on fatigue crack propagation rates, da/dN, in air at 427°C for solution annealed Type 316 stainless steel.

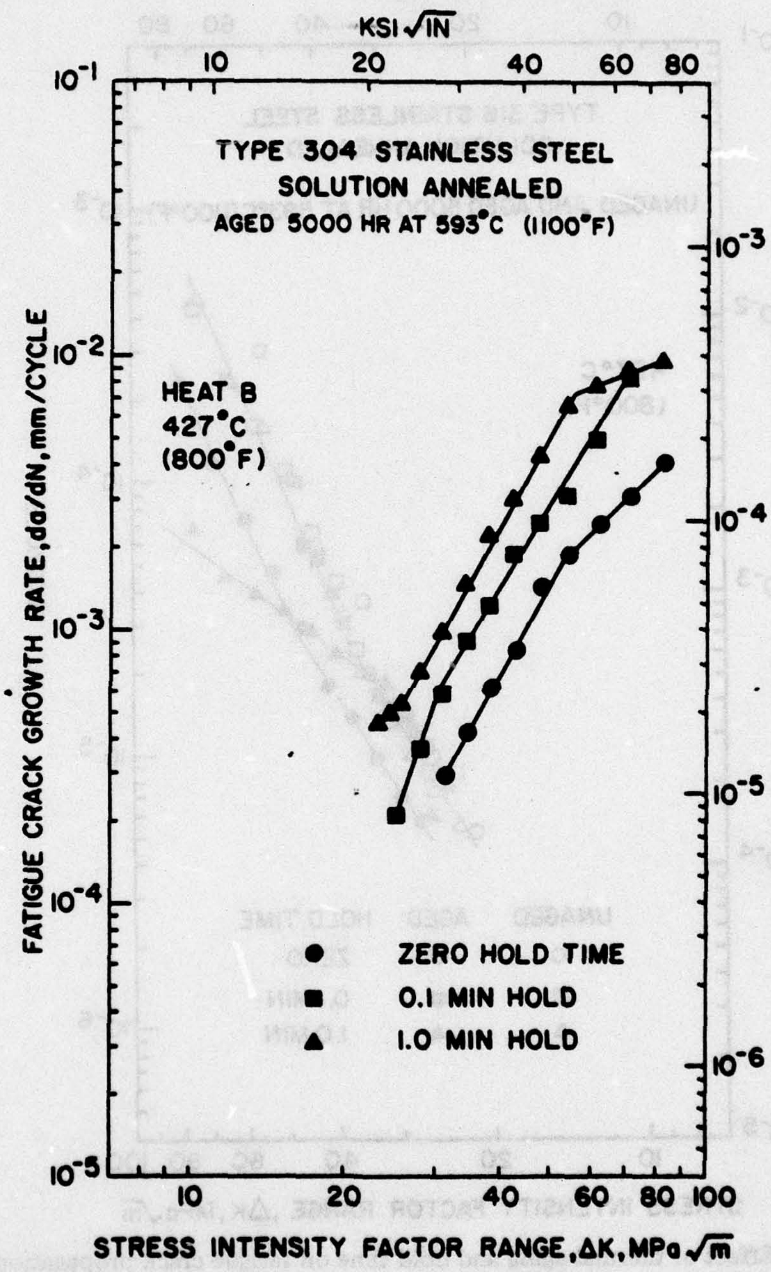

Fig. 5 - Effect of thermal aging and hold time on fatigue crack propagation rates, da/dN, in air at 427°C for solution annealed Type 304 stainless steel (Heat B).

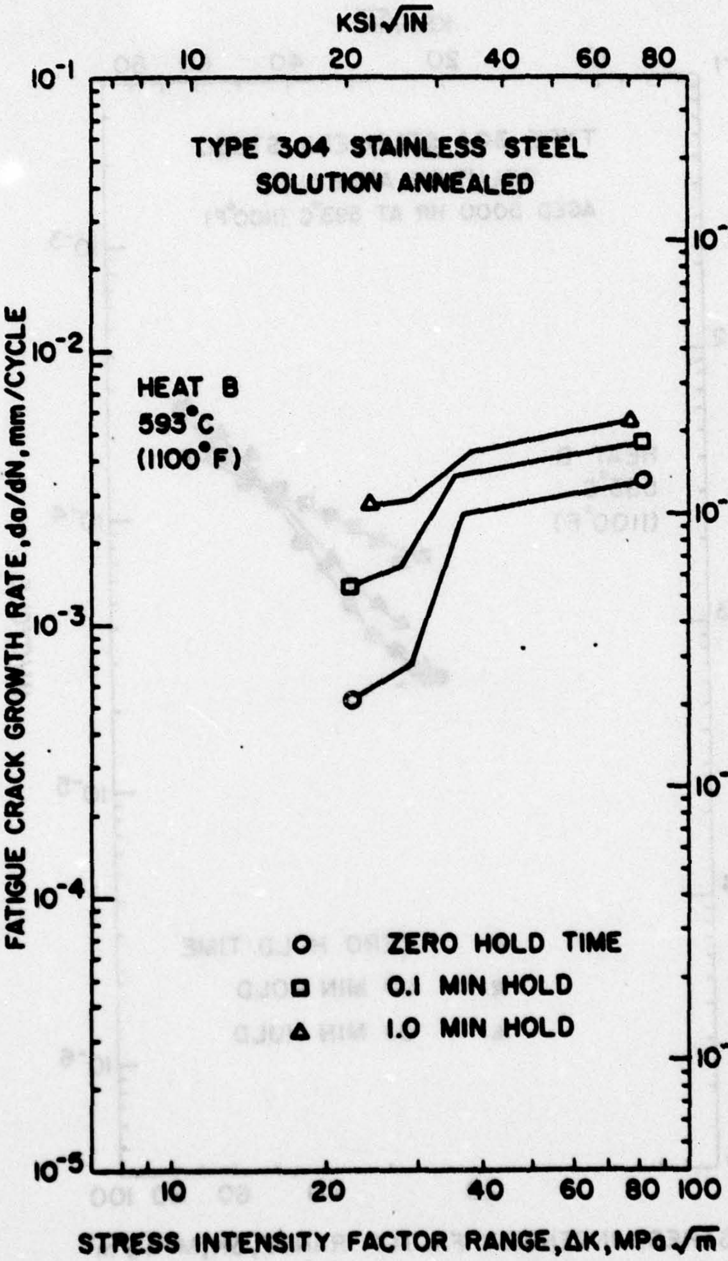

Fig. 6 - Effect of hold time on fatigue crack propagation rates, da/dN, in air at 593°C for unaged, solution annealed Type 304 stainless steel (Heat B), Reference (4).

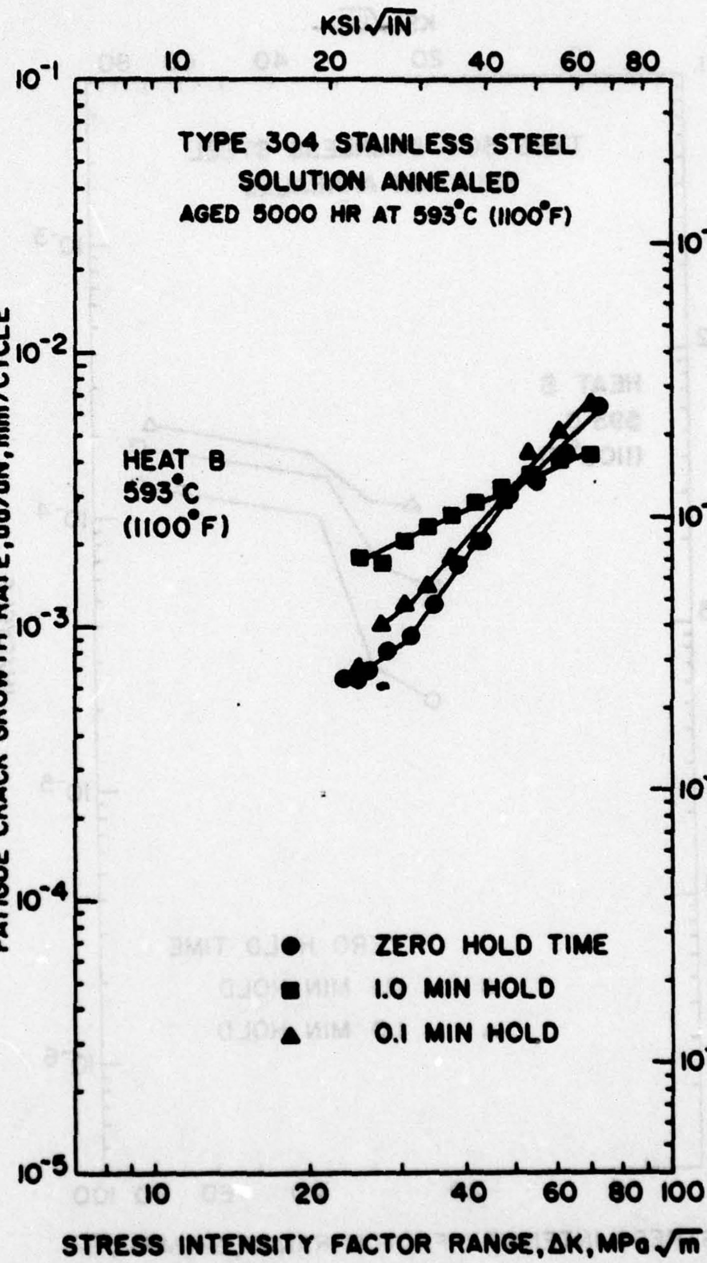

Fig. 7 - Effect of hold time on fatigue crack propagation rates, da/dN, in aid at 593°C for thermally aged, solution annealed Type 304 stainless steel (Heat B).

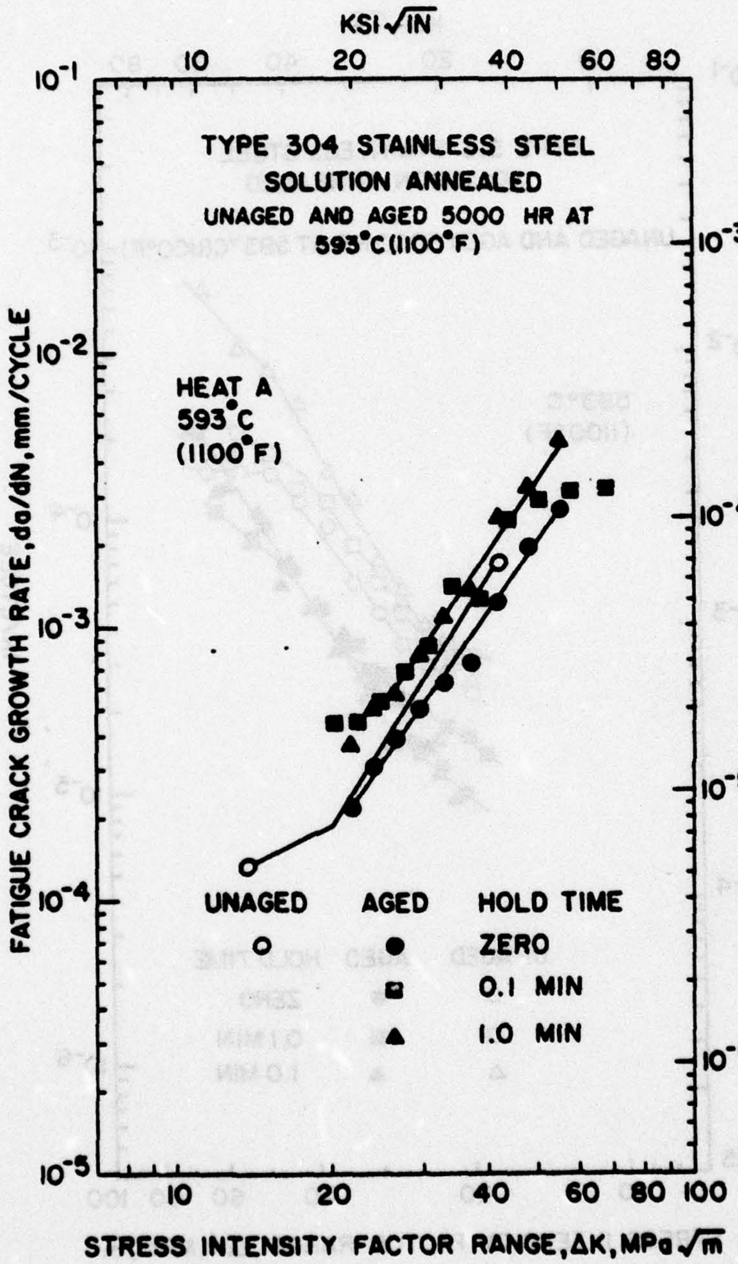

Fig. 8 - Effect of thermal aging and hold time on fatigue crack propagation rates, da/dN, in air at 593°C for solution annealed Type 304 stainless steel (Heat A). The unaged, zero hold time results are those reported by Shahinian, et al. (19).

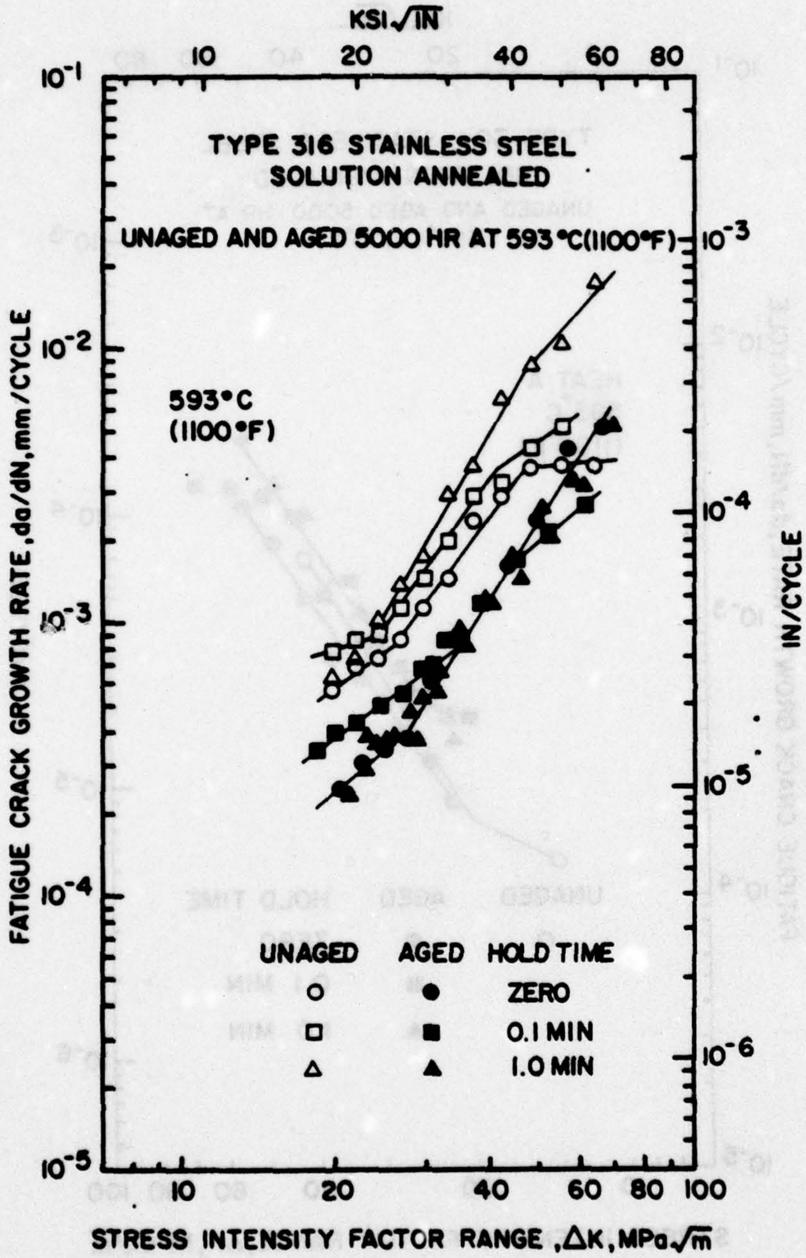

Fig. 9 - Effect of thermal aging and hold time on fatigue crack propagation rates, da/dN, in air at 593°C for solution annealed Type 316 stainless steel.

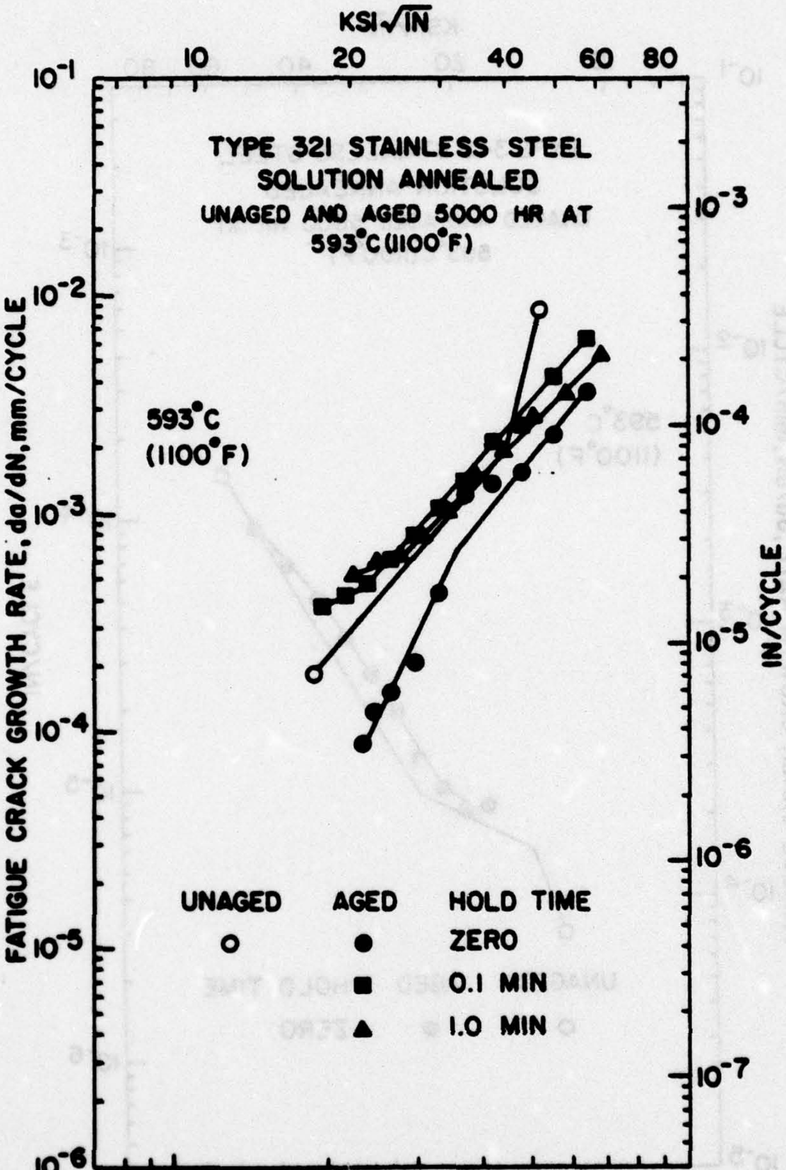

Fig. 10 - Effect of thermal aging and hold time on fatigue crack propagation rates, da/dN, in air at 593°C for solution annealed Type 321 stainless steel. The unaged, zero hold time results are those reported by Shahinian, et al. (19).

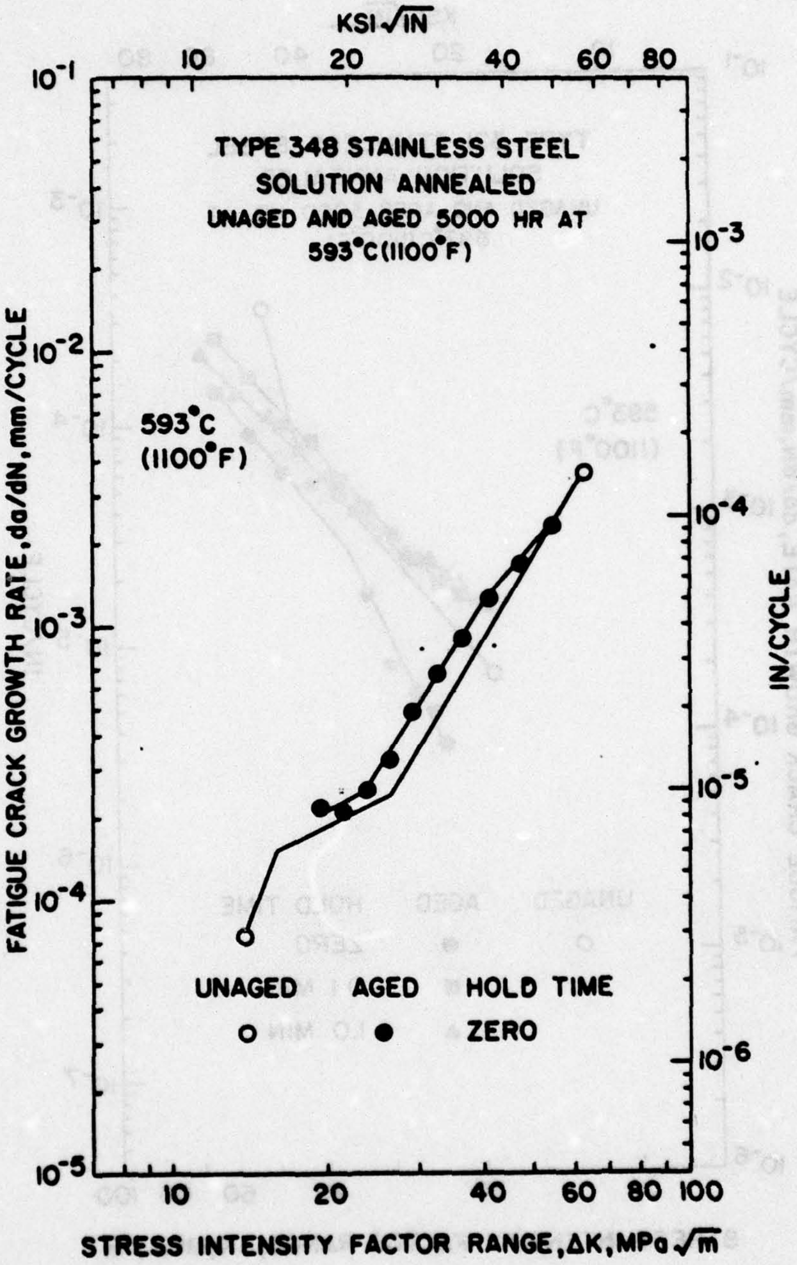

Fig. 11 - Effect of thermal aging on fatigue crack propagation rates, da/dN, in air at 593°C for solution annealed Type 348 stainless steel. The unaged results are those reported by Shahinian, et al. (19).

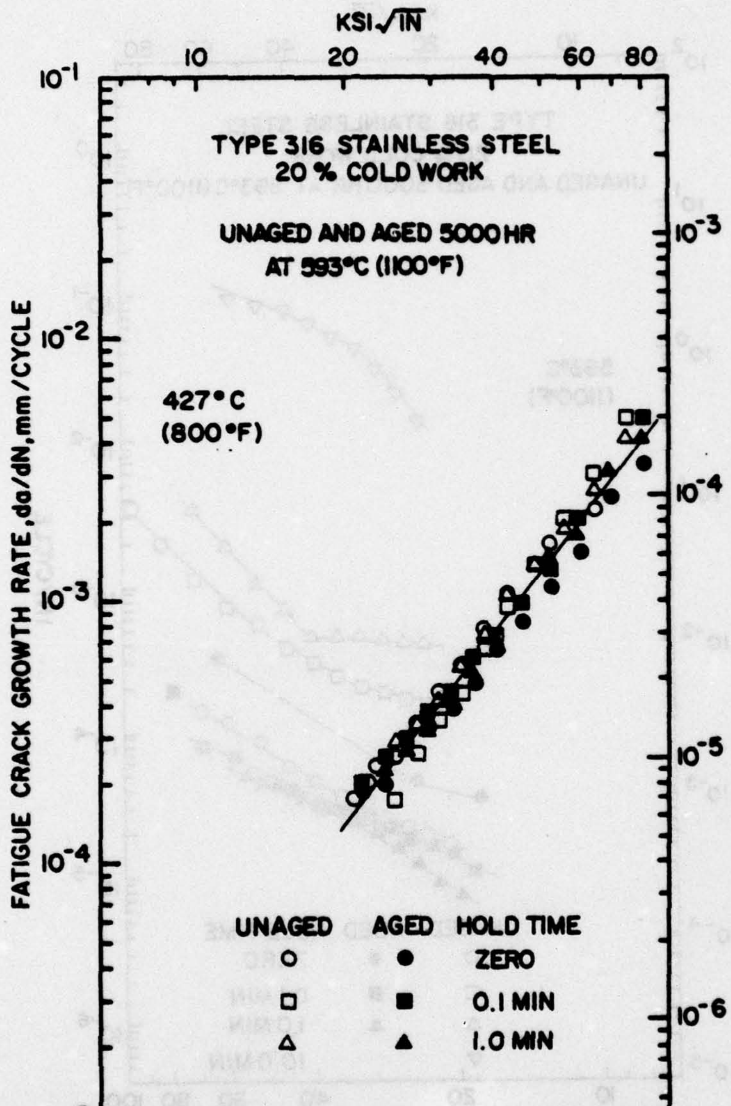

Fig. 12 - Effect of thermal aging and hold time on fatigue crack propagation rates, da/dN, in air at 427°C for 20% cold worked Type 316 stainless steel.

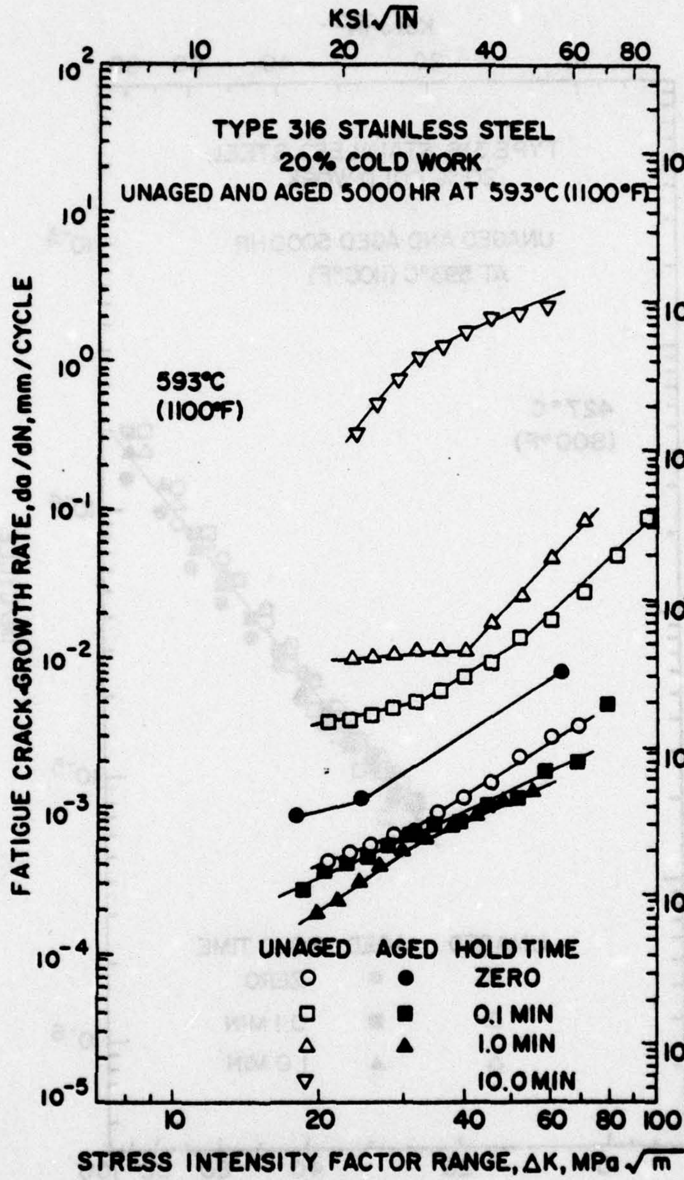

Fig. 13 - Effect of thermal aging and hold time on fatigue crack propagation rates, da/dN, in air at 593°C for 20% cold worked Type 316 stainless steel.

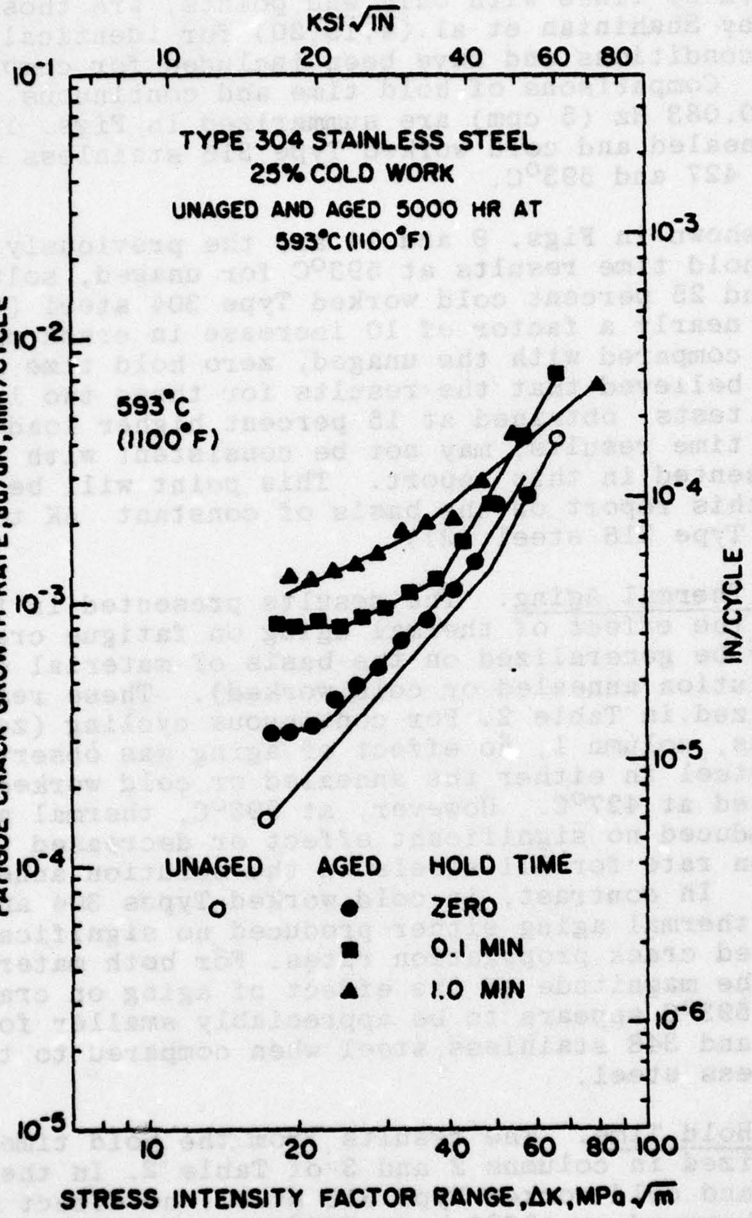

Fig. 14 - Effect of thermal aging and hold time on fatigue crack propagation rates, da/dN, in air at 593°C for 25% cold worked Type 304 stainless steel (Heat A). The unaged, zero hold time results are those reported by Shahinian (20).

crack propagation in cold worked Types 316 and 304 stainless steel at 427 and 593°C. The results in Figs. 4 through 14, represented by lines with only end points, are those previously reported by Shahinian et al.(4,19,20) for identical material and test conditions and have been included for comparison purposes. Comparisons of hold time and continuous cycle results at 0.083 Hz (5 cpm) are summarized in Figs. 15 through 18 for annealed and cold worked Type 316 stainless steel tested at 427 and 593°C.

Not shown in Figs. 9 and 14 are the previously reported 1 minute hold time results at 593°C for unaged, solution annealed, and 25 percent cold worked Type 304 steel (3) which indicated nearly a factor of 10 increase in crack propagation rate when compared with the unaged, zero hold time results. It is now believed that the results for these two 1 minute hold time tests, obtained at 15 percent higher loads than the zero hold time results, may not be consistent with the results presented in this report. This point will be discussed later in this report on the basis of constant ΔK tests at 593°C for Type 316 steel (21).

Effect of Thermal Aging. The results presented in this report show that the effect of thermal aging on fatigue crack propagation may be generalized on the basis of material condition (e.g., solution annealed or cold worked). These results are so summarized in Table 2. For continuous cycling (zero hold time) tests, column 1, no effect of aging was observed for Type 316 steel in either the annealed or cold worked conditions tested at 427°C. However, at 593°C, thermal aging either produced no significant effect or decreased the crack propagation rate for all steels in the solution annealed condition. In contrast, in cold worked Types 304 and 316 material, thermal aging either produced no significant effect or increased crack propagation rates. For both material conditions, the magnitude of the effect of aging on crack propagation at 593°C appears to be appreciably smaller for Type 304, 321, and 348 stainless steel when compared to the Type 316 stainless steel.

Effect of Hold Time. The results from the hold time tests are summarized in columns 2 and 3 of Table 2. In the unaged, annealed, and cold worked Type 316 steel, no effect of hold time was observed at 427°C. At 593°C, in annealed Types 304 and 316 steels, hold time effects were observed and crack growth rates increased with length of the hold period. From column 3, thermal aging did not appear to alter the magnitude of the hold time effects in the solution annealed steels, but in some cases resulting crack growth rates were lower after aging. At 593°C, hold time effects were observed in the unaged, cold worked Type 316 steel and the magnitude of the hold time response was decreased after aging.

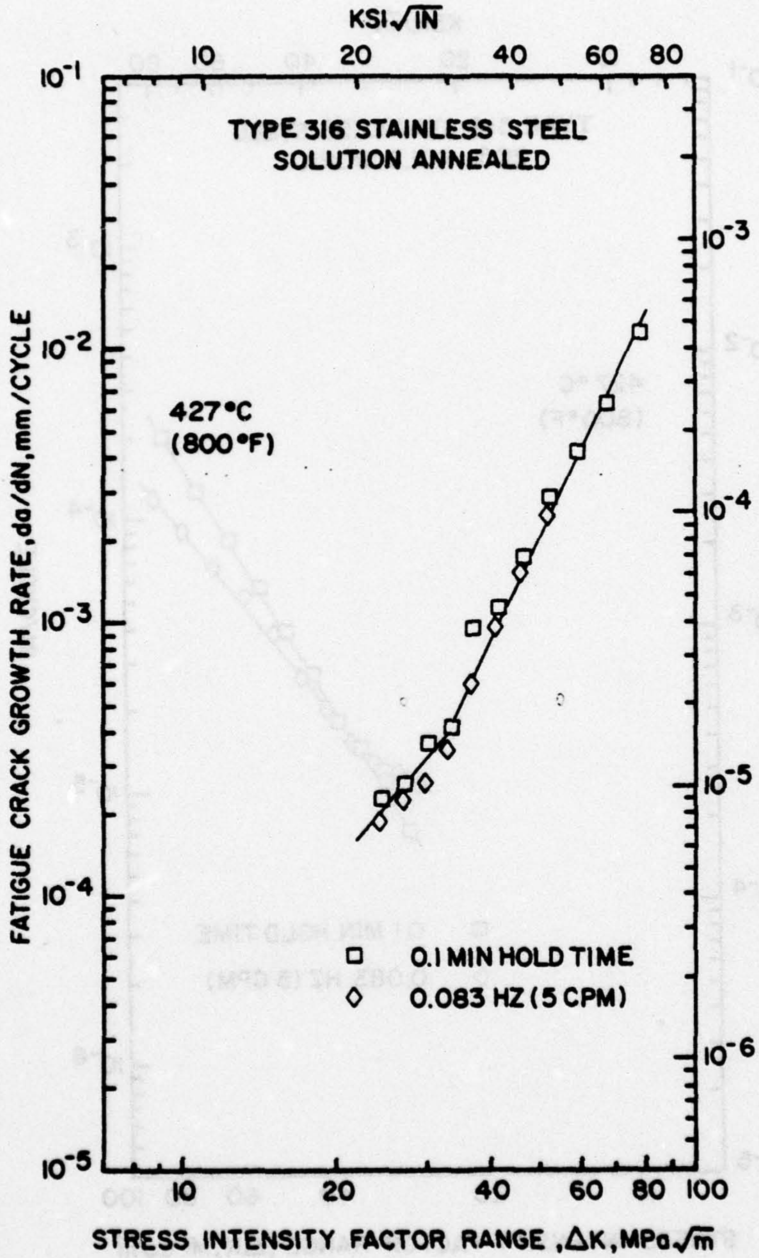

Fig. 15 - Comparison of fatigue crack propagation rates, da/dN, in air at 427°C for solution annealed Type 316 stainless steel produced by continuous 0.083 Hz (5 cpm) cyclic loading and by 0.1 minute hold time.

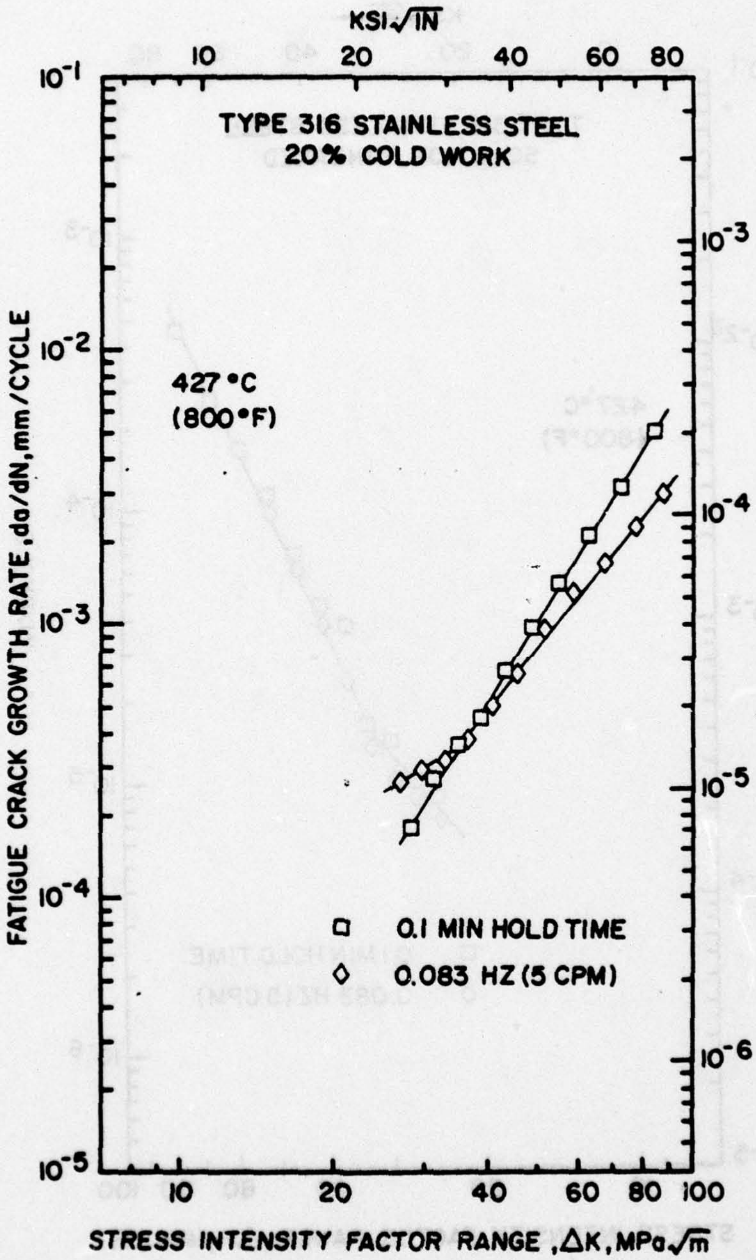

Fig. 16 - Comparison of fatigue crack propagation rates, da/dN, in air at 427°C for 20% cold worked Type 316 stainless steel produced by continuous 0.083 Hz (5 cpm) cyclic loading and by 0.1 minute hold time.

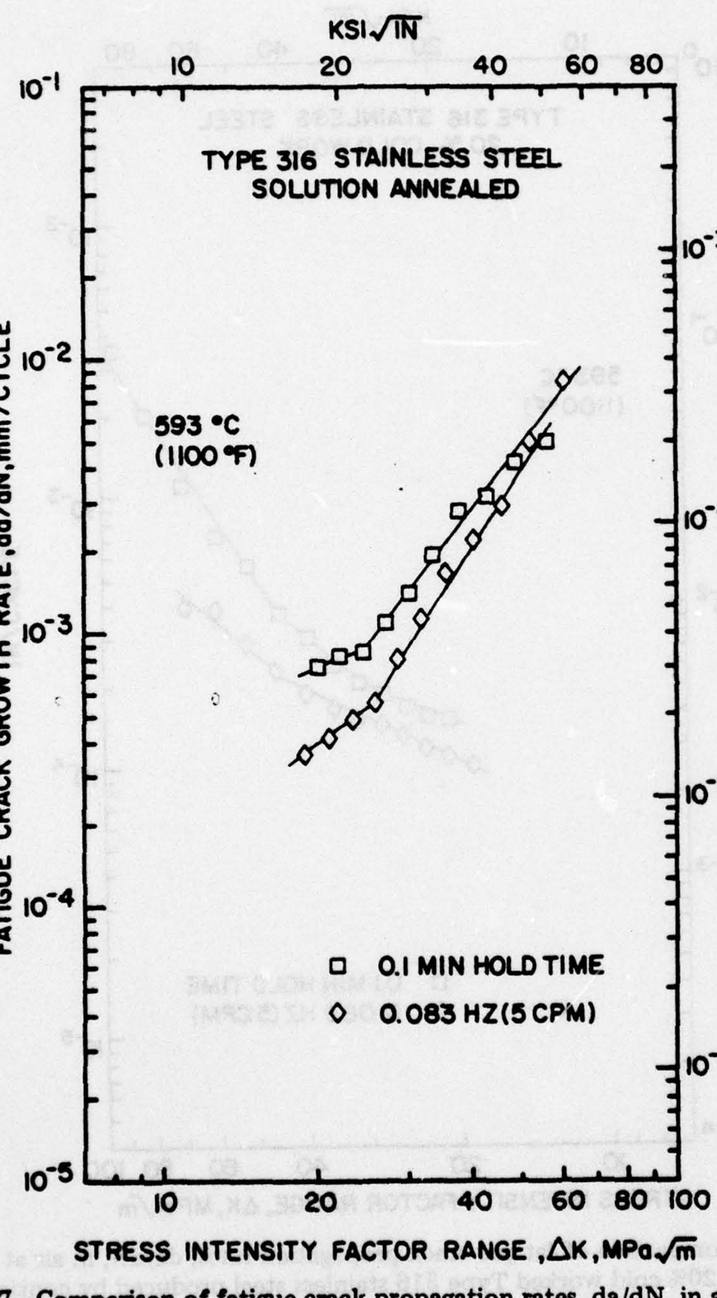

Fig. 17 - Comparison of fatigue crack propagation rates, da/dN, in air at 593°C for solution annealed Type 316 stainless steel produced by continuous 0.083 Hz (5 cpm) cyclic loading and by 0.1 minute hold time.

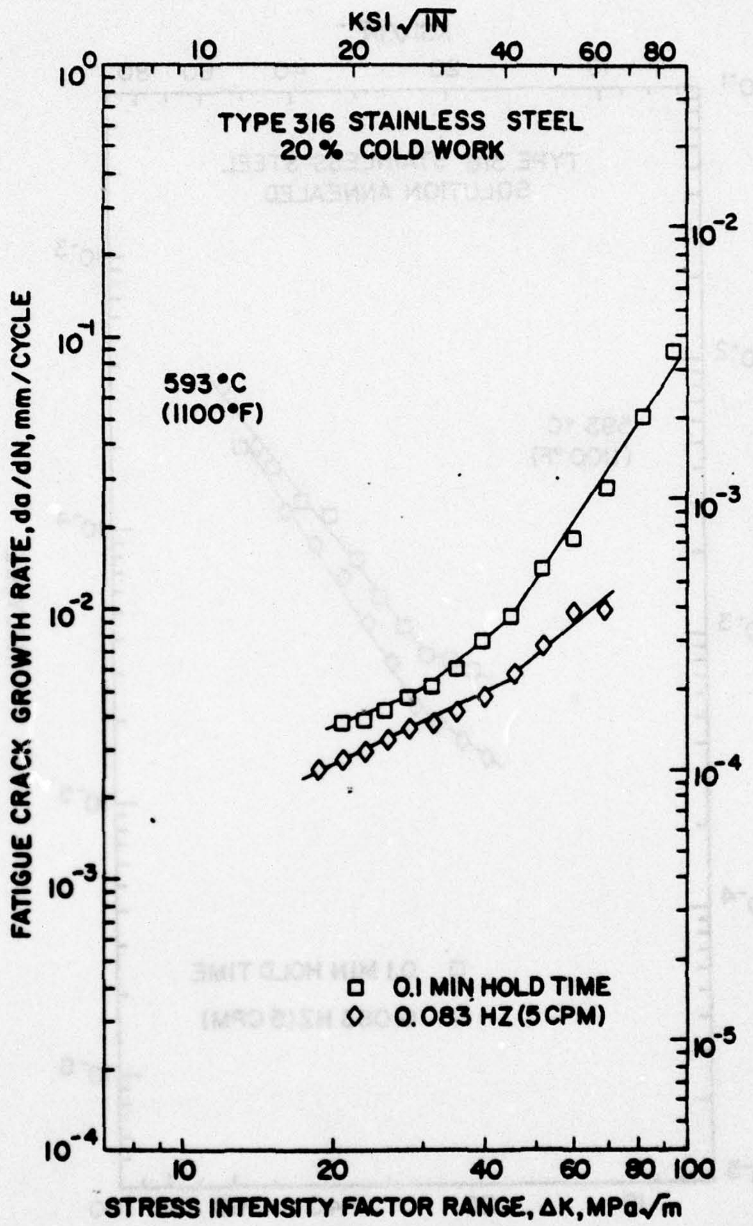

Fig. 18 - *Comparison of fatigue crack propagation rates, da/dN, in air at 593°C for 20% cold worked Type 316 stainless steel produced by continuous 0.083 Hz (5 cpm) cyclic loading and by 0.1 minute hold time.*

TABLE 2

Effect of Aging and Hold Time on Fatigue Crack Propagation Response of Types 304, 316, 321, and 348 Stainless Steel at 427 and 593°C

Material Condition		Effect of Aging (Continuous Cycling)		Effect of Hold Time, Unaged Condition		Effect of Aging on Hold Time	
		427°C	593°C	427°C	593°C	427°C	593°C
SOLUTION ANNEALED	304	-	No Effect	-	Yes	-	No Effect
	316	No Effect	Reduced CGR	No	Yes	No Effect	No Effect
	321	-	Reduced CGR	-	-	-	No Effect
	348	-	No Effect	-	-	-	-
COLD WORKED	304	-	No Effect	-	-	-	-
	316	No Effect	Increased CGR	No	Yes	-	Decreased Hold Time Effect

Hold Time vs. Cyclic Frequency. The relationship between the effect of hold time and reduced cyclic frequency, both of which have been observed to increase elevated temperature crack propagation rate in stainless steels, is not clear. James (22) has concluded that the frequency effects observed in Type 304 stainless steel (23) can be primarily attributed to an interaction of the air environment with the fatigue process rather than to a creep-fatigue interaction. Michel et al. (1) also have discussed this point for 20 percent cold worked Type 316 stainless steel tested at 593°C. On the basis of a da/dt analysis of their results, they concluded that the mechanisms which control crack propagation during hold time and continuous cycling at the same nominal frequency are not necessarily the same.

Further tests have now been completed for Type 316 stainless steel, both solution annealed and 20 percent cold worked at 427 and 593°C, to investigate the relationship between hold time and frequency effects. These results are shown in Figs. 15 through 18. On the basis of da/dN, the results indicate that the crack propagation rate is similar during both 0.083 Hz continuous cycling and 0.1 minute hold time tests at 427°C for both material conditions, Figs. 15 and 16. At 593°C, the results show that the crack propagation rate is higher for the 0.1 minute hold time than for the 0.083 Hz continuous cycling for both material conditions, Figs. 17 and 18. In accord with Michel et al. (1), these results further suggest that the material behavior and mechanisms responsible for the crack propagation during continuous cycling and hold time at the same nominal frequency will be different at 593°C despite environmental interaction effects. Additional work is now underway by the authors to clarify these points through characterizations of the fatigue substructure and fracture appearance of the purely cyclic and hold-time specimens.

Hardness

One indication of the relationship between microstructure and properties of materials is hardness. The hardness values determined for the Types 304 and 316 stainless steels used in this study are given in Table 3. The results show that the effect of thermal aging is to produce a bulk hardening in the solution annealed material and a slight reduction in hardness in the cold worked material. These results are entirely consistent with the fatigue crack propagation results; that is, for the purely cyclic loading condition, crack propagation rates are generally reduced in the annealed materials and increased in the cold materials. However, the most significant effect of the aging is the overall reduction in the magnitude of the hold time effects observed for the cold worked Type 316 stainless steel at 593°C.

TABLE 3

Brinell Hardness of Types 304 and 316 Stainless Steels Tested at 593°C (1100°F)

MATERIAL	CONDITION		BRINELL HARDNESS NUMBER
Type 304 (Heat B)	Solution Annealed	Unaged	138
		Thermally* Aged	146
Type 304 (Heat A)	Solution Annealed	Unaged	146
		Thermally* Aged	156
	25% Cold Worked	Unaged	269
		Thermally* Aged	248
Type 316	Solution Annealed	Unaged	144
		Thermally* Aged	158
	25% Cold Worked	Unaged	236
		Thermally* Aged	228

*5000 hours at 593°C (1100°F)

Microscopy

Transmission electron microscopy (TEM) of the Type 316 stainless steel specimens illustrates the effects of the thermal aging on the solution annealed and cold worked microstructures. In the annealed material, Fig. 19 shows that the primary effect of aging was the precipitation of $M_{23}C_6$ carbides which occurred at the grain boundaries. Carbide precipitates also are seen within the matrix where grain boundaries migrated away from their former positions. Somewhat smaller $M_{23}C_6$ precipitates were formed in the cold worked material at the grain boundaries during aging as well as within the grains on the deformation bands, Fig. 20. As previously reported (3), the thermal aging also promoted recovery of the cold worked dislocation substructure. Similar microstructures have been obtained for the Type 304 stainless steels used in this study.

Scanning electron microscopy (SEM) was used to examine the fracture mode of the tested Type 316 stainless steel crack propagation specimens. The micrographs show that the fracture mode was primarily transgranular at 427°C, regardless of hold time and/or thermal aging, for both the solution annealed and cold worked conditions. However, as previously reported (3) at 593°C, Fig. 21 indicates that with increased hold time the fracture mode was intergranular in the unaged, solution annealed material while remaining transgranular at all hold times in the thermally aged material. Results similar to those in Fig. 21 are seen in Fig. 22 for the 20 percent cold worked Type 316 stainless steel. A more detailed examination of these specimens is now in progress and will be reported in a subsequent paper.

DISCUSSION

Interpretation of the effects of thermal aging and hold time on fatigue crack propagation performance requires examination of the various mechanisms likely to be effective in controlling the crack propagation process in these alloys. For this purpose, the results from the microscopic evaluation of the failure mode and microstructure of the test specimens will be considered along with the hardness results and environmental factors. Finally, these tests for Type 304 steel, previously noted to be inconsistent, will be discussed on the basis of evidence derived from constant ΔK tests conducted to evaluate load dependence during hold time.

Examination of the hardness results for both Type 304 and 316 steel as well as the SEM results for the Type 316 steel suggests that the primary influence of the precipitates produced by thermal aging was to increase the hardness of

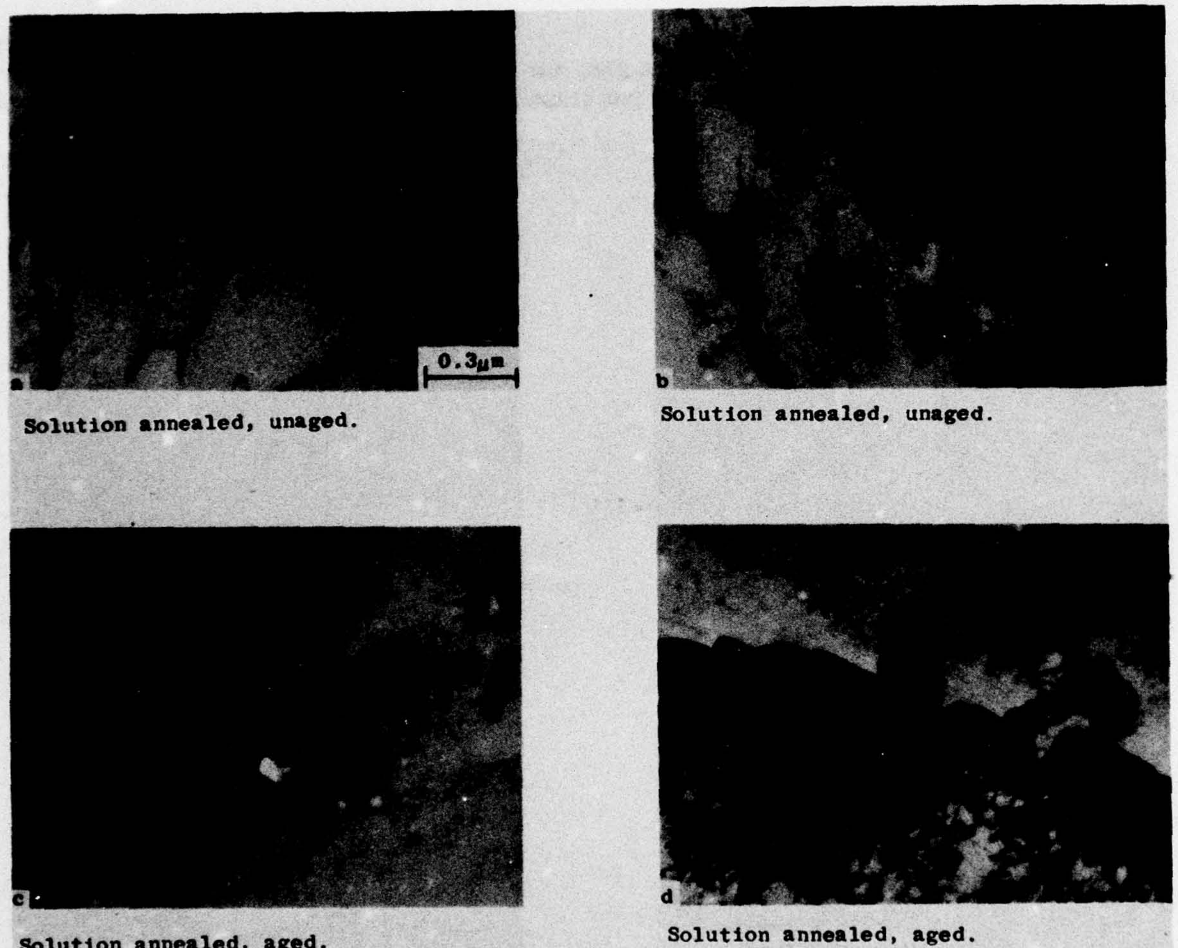

Fig. 19 - TEM micrographs of dislocation substructure and grain boundaries in aged and unaged, solution annealed Type 316 stainless steel. Aged material was held at 593°C for 5000 hours prior to crack propagation testing.

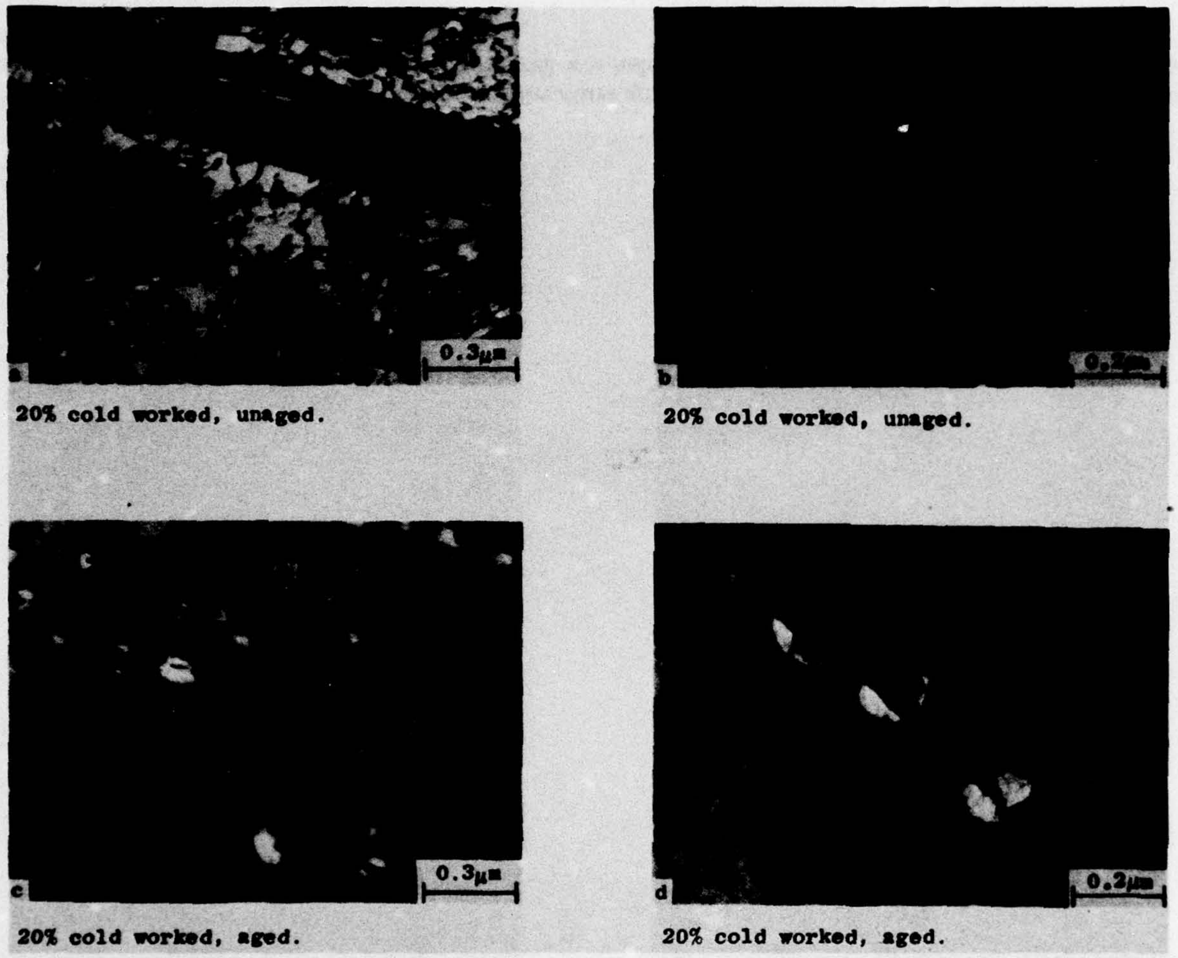

Fig. 20 - TEM micrographs of dislocation substructure and grain boundaries in aged and unaged, 20% cold worked Type 316 stainless steel. Aged material was held at 593°C for 5000 hours prior to crack propagation testing.

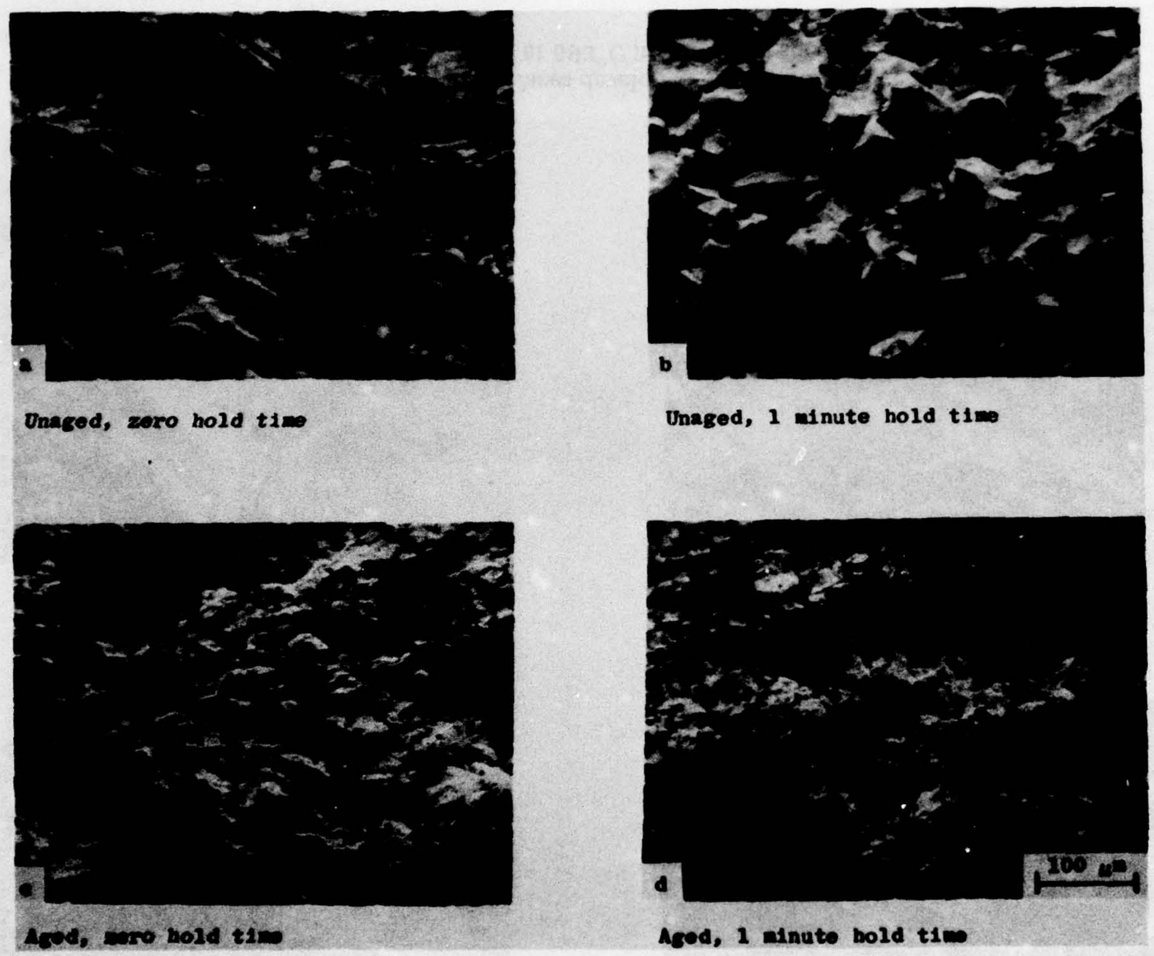

Fig. 21 - SEM micrographs of fracture surfaces developed during the fatigue of aged and unaged, annealed Type 316 stainless steel at 593°C in air. Aged specimens were held at 593°C for 5000 hours, $\Delta K \approx 25\ MPa\sqrt{m}$.

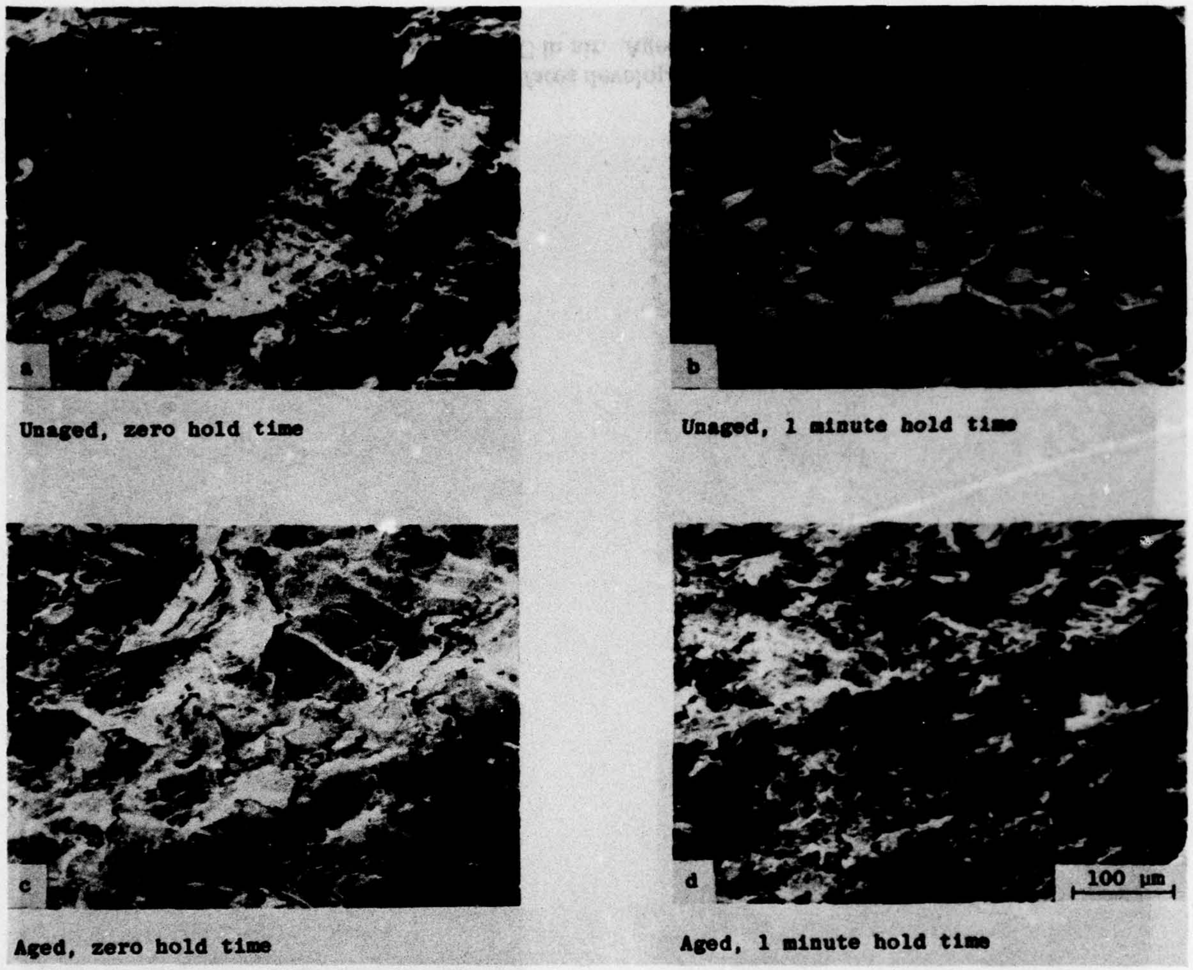

Fig. 22 - SEM micrographs of fracture surfaces developed during the fatigue of aged and unaged, 20% cold worked Type 316 stainless steel at 593°C in air. Aged specimens were held at 593°C for 5000 hours, $\Delta K \approx 25\ MPa\sqrt{m}$.

both steels in the solution annealed condition and to alter the rate and mode of crack propagation with increased hold time at 593°C. However, it is evident from the TEM results that the majority of the precipitate formation in solution annealed Type 316 steel occurred in the grain boundaries. In the cold worked Type 316 steel, the results in Fig. 20 illustrate that smaller precipitates were formed in the grain boundaries as well as along the deformation bands within the matrix. For the solution annealed conditions, then, it is the precipitates formed during aging which contribute to the increased hardness and the improved crack propagation resistance at 593°C. The product of the competing mechanisms of aging and thermal recovery results in a bulk softening and slightly reduced crack propagation resistance in the cold worked Type 316 stainless steel.

The transition from transgranular to intergranular fracture mode with increased hold time, as shown in the SEM micrographs in Figs. 21 and 22, suggests that a grain boundary cavity and/or sliding mechanism was active during the hold time tests at 593°C in Type 316 steel. This is reasonable since it is known that, at temperatures near approximately one-half the melting point ($0.5\ T_m$), intergranular cavity formation produced by grain boundaries sliding is a prominent *deformation mechanism during both creep and fatigue.* However, it is also well known that test environment can have a pronounced effect on fatigue crack propagation in austenitic stainless steels (24). Recent work has shown that grain boundary oxide penetration can occur ahead of the crack in stainless steels and be followed by intergranular crack formation suggesting that oxygen diffusion ahead of the crack could be important to the propagation process (25). Based on SEM observations of the fracture surfaces of the unaged, solution annealed Type 316 stainless steel specimens tested at 593°C in the present study, Smidt and Provenzano concluded (26) that the increased tendency for an intergranular failure mode with increased hold time was consistent with conditions where the penetration distance of oxygen diffusion along the grain boundaries exceeds the crack propagation rate per cycle. Nevertheless, Solomon and Coffin (27) have shown that the transition from a transgranular to an intergranular failure mode in fatigue occurs in both vacuum and in air environments, except that the cyclic frequency is shifted to lower values in vacuum. The oocurrence of the transition in vacuum provides direct evidence that it is related to the basic material behavior rather than to the environment. The effect of the air environment, then, is to simply accelerate the transition from transgranular to intergranular failure mode rather than changing the basic physical mechanisms of elevated temperature crack propagation. It is proposed, therefore, that a grain boundary sliding mechanism, possibly influenced by environmental attack, was primarily responsible for the hold time effects on fatigue crack propagation observed experimentally in this study in the unaged, solution annealed Type 316 stainless steel. Furthermore, it is proposed that the effect of the intergranular precipitates produced by thermal aging was to suppress the grain boundary sliding and oxygen diffusion to delay the transition in failure mode from transgranular to intergranular until the rate of crack advance by creep (or creep-like) mechanisms exceeded that by fatigue mechanisms.

The proposed mechanism by which intergranular precipitates in the thermally aged Type 316 stainless steel influence crack propagation has been previously incorporated into a hypothesis by Michel and Smith (28) concerning the overall effects of intergranular precipitates on crack propagation in air. Their hypothesis, that the effect of the intergranular precipitates in aged, solution annealed Type 316 stainless steel is to simply delay the transition in fracture mode from transgranular to intergranular with increased hold time by the suppression of grain boundary sliding (which occurs during the hold periods due to localized stress relaxation and leads to cavity formation) and, hence, the intergranular infiltration of oxygen, has been verified by their recent experimental results (29) during crack propagation tests with hold times longer than one minute at 593°C. These results show that the transition to an intergranular fracture mode actually occurs at a hold time of 16 minutes whereas the unaged material exhibits an intergranular fracture mode at a hold time of only one minute. Despite the experimental results (Fig. 13) which show that thermal aging increased the crack propagation rate in 20 percent cold worked material at 593°C during zero hold time tests, the observation that thermal aging suppressed the effects of hold time on crack propagation rate suggests that a mechanism similar to that proposed for the effect of thermal aging on the solution annealed steel may apply to the cold worked materials as well. Experiments for cold worked material, complementary to those being conducted for the aged, solution annealed material, are in progress at hold times longer than one minute to ascertain the responsible mechanism.

The methods employed for the analysis of the fatigue crack propagation results in this report were those of linear elastic fracture mechanics (LEFM). These methods require that the crack propagation be independent of load at a constant value of the stress intensity factor. Although the experimental results generally show good agreement on the basis of these methods, it is reasonable to expect that fracture mechanics parameters may not apply under conditions where time dependent deformation processes may become active, such as during hold time tests at 593°C.

With the exception of the two previously noted 1 minute hold time tests for solution annealed and 25 percent cold worked Type 304 stainless steel at 593°C, all tests at this temperature were conducted at a load of 3.1×10^3 N (700 pounds). These two tests for Type 304 stainless steel, which were conducted at a load of $\sim 4.0 \times 10^3$ N ($\sim$900 pounds), show significantly higher crack propagation rates than would be expected on the basis of the results for Type 316 stainless steel at 593°C with 1 minute hold time at loads of 3.1×10^3 N (700 pounds).

The relationship between crack propagation rate, hold time, and load has been investigated by Smith and Michel (21) for solution annealed Type 316 steel at 593°C. Their results show that, at loads above $\sim 3.1 \times 10^3$ N (700 pounds), the crack propagation rate during hold time tests are non-linear at a constant ΔK of 32.9 $MPa\sqrt{m}$ (30 $ksi\sqrt{in.}$) whereas the continuous cycling results were linear indicating load independence to $\sim 6 \times 10^3$ N ($\sim$1350 pounds). These results confirm that the tests for the Type 304 stainless steel conducted at a load of $\sim 4.0 \times 10^3$ N ($\sim$900 pounds) are inconsistent with LEFM criteria. However, the remainder of the hold time crack propagation results given in this report were generated under the experimental conditions consistent with the load independence criteria and are, therefore, comparable with the zero hold time results on the basis of stress intensity factor range.

SUMMARY AND CONCLUSIONS

The effects of thermal aging and hold time on fatigue crack propagation of Types 316, 304, 321, and 348 stainless steel were investigated at 427 and 593°C (800 and 1100°F). The following conclusions are drawn from the results.

1. Tensile hold periods of 0.1 and 1.0 minutes have no significant effect on crack propagation rate in unaged or thermally aged, annealed and 20 percent cold worked Type 316 stainless steel at 427°C. A small effect of hold time was observed in thermally aged Type 304 stainless steel at 427°C.

2. At 593°C, thermal aging produced no significant effect on crack propagation rate during continuous cycling for annealed and cold worked Type 304 stainless steel and annealed Type 348 stainless steel.and reduced the crack propagation rate in annealed Types 316 and 321 stainless steel.

3. In the unaged condition, 0.1 and 1.0 minute hold times at 593°C increased the crack propagation rate for annealed Types 304 and 316 stainless steel and for 20 percent cold worked Type 316 stainless steel.

4. In the thermally aged condition, 0.1 and 1.0 minute hold times at 593°C produced no significant effect on crack propagation rate for solution annealed Types 304, 316, and 321 stainless steel and reduced the crack propagation rate for 20 percent cold worked Type 316 stainless steel.

5. The microstructural effects of thermal aging at 593°C were the production of massive intergranular $M_{23}C_6$ precipitates as well as smaller, more widely dispersed matrix precipitates in solution annealed Type 316 stainless steel. In 20 percent cold worked material, thermal aging at 593°C produced smaller intergranular $M_{23}C_6$ precipitates as well as matrix precipitates on deformation bands.

6. The failure mode of solution annealed and 20 percent cold worked Type 316 stainless steel at 593°C was found to be transgranular during continuous cycling (zero hold time) and intergranular at hold times of 1 minute. In thermally aged material, the failure mode was transgranular regardless of hold time (zero, 0.1, and 1.0 minutes).

7. It is concluded that the mechanism by which the intergranular precipitates influenced crack propagation performance and failure mode of aged, solution annealed Type 316 stainless steel at 593°C is the suppression of grain boundary sliding, and any associated environmental interaction, to delay the transition in failure mode from transgranular to intergranular until the rate of crack advance by creep (or creep-like) mechanisms exceeded that by fatigue mechanisms.

ACKNOWLEDGMENTS

This research was supported by the Office of Naval Research and the Energy Research and Development Administration. The authors gratefully acknowledge the experimental assistance of J. T. Atwell and E. Woodall. The assistance of G. R. Evers in the development of the calculator program for processing the fatigue data and in the preparation of the description of the program in the Appendix is gratefully acknowledged.

REFERENCES

1. D. J. Michel, H. H. Smith, and H. E. Watson, "Effect of Hold Time on Elevated Temperature Fatigue Crack Propagation in Fast Neutron Irradiated and Unirradiated Type 316 Stainless Steel," in Structural Materials for Service at Elevated Temperatures in Nuclear Power Generation, A. O. Schaefer, Ed., American Society of Mechanical Engineers, MPC-1, 1975, pp. 167-190.

2. D. J. Michel and H. H. Smith, "Effect of Thermal Aging and Hold Time on Fatigue Crack Propagation in Type 316 Stainless Steel," in Proceedings of the Second International Conference on Mechanical Behavior of Materials, American Society for Metals, 1976, pp. 568-572.

3. D. J. Michel and H. H. Smith, "Crack Growth Behavior Under Creep Fatigue Conditions in Alloy 718," in 1976 ASME-MPC Symposium on Creep-Fatigue Interaction, R. M. Curran, Ed., American Society of Mechanical Engineers, MPC-3, 1976, pp. 391-415.

4. P. Shahinian, "Creep-Fatigue Crack Propagation in Austenitic Stainless Steel," J. Pressure Vessel Technology, Trans. ASME, Vol. 98, 1976, pp. 166-172.

5. R. D. Nicholson, "The Effect of Temperature on Creep Crack Propagation in AISI Type 316 Stainless Steel," Mater. Sci. Eng., Vol. 22, 1976, p. 1.

6. J. Wareing, "Creep-Fatigue Interaction in Austenitic Stainless Steels," Metallurgical Transactions, Vol. 8A, 1977, pp. 711-721.

7. P. Shahinian, "Crack Propagation in Cold Worked Austenitic Stainless Steel at Elevated Temperatures," submitted for publication, 1977.

8. B. Weiss and R. Stickler, "Phase Instabilities During High Temperature Exposure of 316 Austenitic Stainless Steel," Metallurgical Transactions, Vol. 3, 1972, pp. 851-866.

9, J. E. Spruiell, J. A. Scott, C. S. Ary, and R. L. Hardin, "Microstructural Stability of Thermal Mechanically Pretreated Type 316 Austenitic Stainless Steel," Metallurgical Transactions, Vol. 4, 1973, pp. 1533-1544.

10. F. Garofalo, F. Von Gemmingen, and W. F. Domis, "The Creep Behavior of an Austenitic Stainless Steel as Effected by Carbides Precipitates on Dislocations," Trans. ASM, Vol. 54, 1961, p. 430.

11. J. T. Barnby and F. M. Peace, "The Effects of Carbides on the High Strain Fatigue Resistance of an Austenitic Steel," Acta Met., Vol. 19, 1971, p. 1351.

12. J. T. Barnby and F. M. Peace, "Influence of Carbides on the Low-Cycle Fatigue Strength of an Austenitic Steel," in Effect of Second-Phase Particles on the Mechanical Properties of Steel, The Iron and Steel Institute, London, 1971, p. 124.

13. J. H. Driver, "The Effect of Boundary Precipitates on the High-Temperature Fatigue Strength of Austenitic Stainless Steels," Met. Sci. Journal, Vol.5, 1971, p.47.

14. L. A. James, "Effect of Thermal Aging Upon the Fatigue-Crack Propagation of Austenitic Stainless Steels," Metallurgical Transactions, Vol. 5, 1974, pp. 831-838.

15. P. Shahinian, H. E. Watson, and H. H. Smith, "Effect of Neutron Irradiation on Fatigue Crack Propagation in Types 304 and 316 Stainless Steels at High Temperatures," in Effects of Radiation on Substructure and Mechanical Properties of Metals and Alloys, ASTM STP 529, American Society for Testing and Materials, 1973, pp. 493-508.

16. B. Gross and J. E. Srawley, "Stress-Intensity Factors for Single-Edge-Notch Specimens in Bending or Combined Bending and Tension by Boundary Collocation of a Stress Function," NASA-TN-D2603, National Aeronautics and Space Administration, Washington, D.C., January 1965.

17. 1973 Annual Book of ASTM Standards, Standard Recommended Practice E10-66, Part 31, American Society for Testing and Materials, Philadelphia, Pa., 1973.

18. D. J. Michel, J. Moteff, and A. J. Lovell, "Substructure of Type 316 Stainless Steel Deformed in Slow Tension at Temperatures Between 21 and 816°C," Acta Met., Vol. 21, 1973, pp. 1269-1277.

19. P. Shahinian, H. H. Smith, and H. E. Watson, "Fatigue Crack Growth Characteristics of Several Austenitic Stainless Steels at High Temperatures," in Fatigue at Elevated Temperatures, ASTM 520, American Society for Testing and Materials, 1973, pp. 387-397.

20. P. Shahinian, "Fatigue Crack Propagation in Fast Neutron Irradiated Stainless Steels and Welds," in Properties of Reactor Structural Alloys After Neutron or Particle Irradiation, ASTM 570, American Society for Testing and Materials, 1975, pp. 191-204.

21. H. H. Smith and D. J. Michel, "Fatigue Crack Propagation in Type 316 Stainless Steel at Elevated Temperatures," Report of NRL Progress, October 1976, pp. 7-8; unpublished results, 1977.

22. L. A. James, "Frequency Effects in the Elevated Temperature Crack Growth Behavior of Austenitic Stainless Steels-A Design Approach," HEDL-SA-1342, Hanford Engineering Development Laboratory, Richland, WA., August 1977.

23. L. A. James, "Hold-Time Effects on the Elevated Temperature Fatigue-Crack Propagation of Type 304 Stainless Steel," Nucl. Technology, Vol. 16, 1972, pp. 521-530.

24. H. H. Smith, P. Shahinian, and M. R. Achter, "Fatigue Crack Growth Rates in Type 316 Stainless Steel at Elevated Temperature as a Function of Oxygen Pressure," Trans. Met. Soc. of AIME, Vol. 245, 1969, pp. 947-953.

25. L. F. Coffin, "Fatigue at High Temperature-Prediction and Interpretation," Proc. Inst. Mech. Engrs., Vol. 188, 1974, p. 109.

26. F. A. Smidt, Jr. and V. E. Provenzano, "SEM Observations of Fracture Surfaces of Fatigue Specimens of Annealed Type 316 Stainless Steel," NRL Report 8133, Naval Research Laboratory, Washington, D.C., August 10, 1977.

27. H. D. Solomon and L. F. Coffin, Jr., "Effects of Frequency and Environment on Fatigue Crack Growth in A286 at 1100 F," in Fatigue at Elevated Temperatures, ASTM STP 520, American Society for Testing and Materials, 1973, pp. 112-122.

28. D. J. Michel and H. H. Smith, J. Engr. Matls. and Tech., Trans. ASME, Series H, Vol. 99, 1977, p. 282.

29. D. J. Michel and H. H. Smith, unpublished results, Naval Research Laboratory, 1977.

APPENDIX A

Description of Calculator Program for Processing, Storage and Retrieval of Fatigue Crack Propagation Data

A versatile program has been developed for processing fatigue crack propagation data using a Hewlett-Packard 9830A Calculator equipped with the following accessories: six ROM (Read-Only-Memory) options, a thermal line printer, plotter, paper tape reader, and magnetic cassette tape recorder. Calculator specifications include: a core memory of 3808 words, data storage of more than 32,000 words, and a bi-directional search speed of 130 ft (magnetic tape) per minute.

The fatigue crack propagation data processing program incorporates three separate sub-programs to aid in the reduction, analysis, plotting, storage, and retrieval of both new and previously reported test data. The essential features of the program are shown schematically in the flow diagram in Fig. A-1. A brief description of each sub-program is included in the following paragraphs.

A. Crack Length (a) versus Cycles (N) Data

Experimental data taken during the fatigue crack propagation tests are entered either manually via the keyboard or via punched paper tape, up to a maximum of 200 points. The program inputs and plots each data point. The crack length (a) versus number of cycles (N) data are then fitted to a smooth curve. Points taken from this smooth curve provide the input to the subsequent da/dN versus ΔK analysis.

B. Crack Propagation Rate (da/dN) versus Stress Intensity Factor Range (ΔK) Calculation

This sub-program has the option of data file manipulation allowing specific placement of new test results. Data may be entered either as a versus N, or as da/dN versus ΔK. Once a form has been selected for input, the data are transferred with all necessary accompanying information directly to memory by keyboard or paper tape. Computations are then performed by the program applicable to the original entered form, which can be printed, stored, and plotted.

C. Retrieval of Stored Data

Each specimen can be listed with its concommitant parameters for specific data selection and analysis. Once a file has been chosen, the data are retrieved from storage and plotted.

The computation of the crack propagation rate, da/dN, and the stress intensity factor range, ΔK, performed in the sub-programs are accomplished in the following manner. The crack propagation rate is computed from the a vs. N data according to the following slopes expression:

$$da/dN = (a_{n+1} - a_n)/(N_{n+1} - N_n), \qquad \text{(A-1)}$$

where a and N are crack length and cycles, respectively, and n is sequential number of each pair of a vs. N data. The da/dN value represents the crack propagation rate at the midpoint of each two pairs of a vs. N data. The stress intensity factor range, ΔK, is computed according to the equation given by Gross and Srawley (16) for single-edge-notched (SEN) cantilevel specimens.

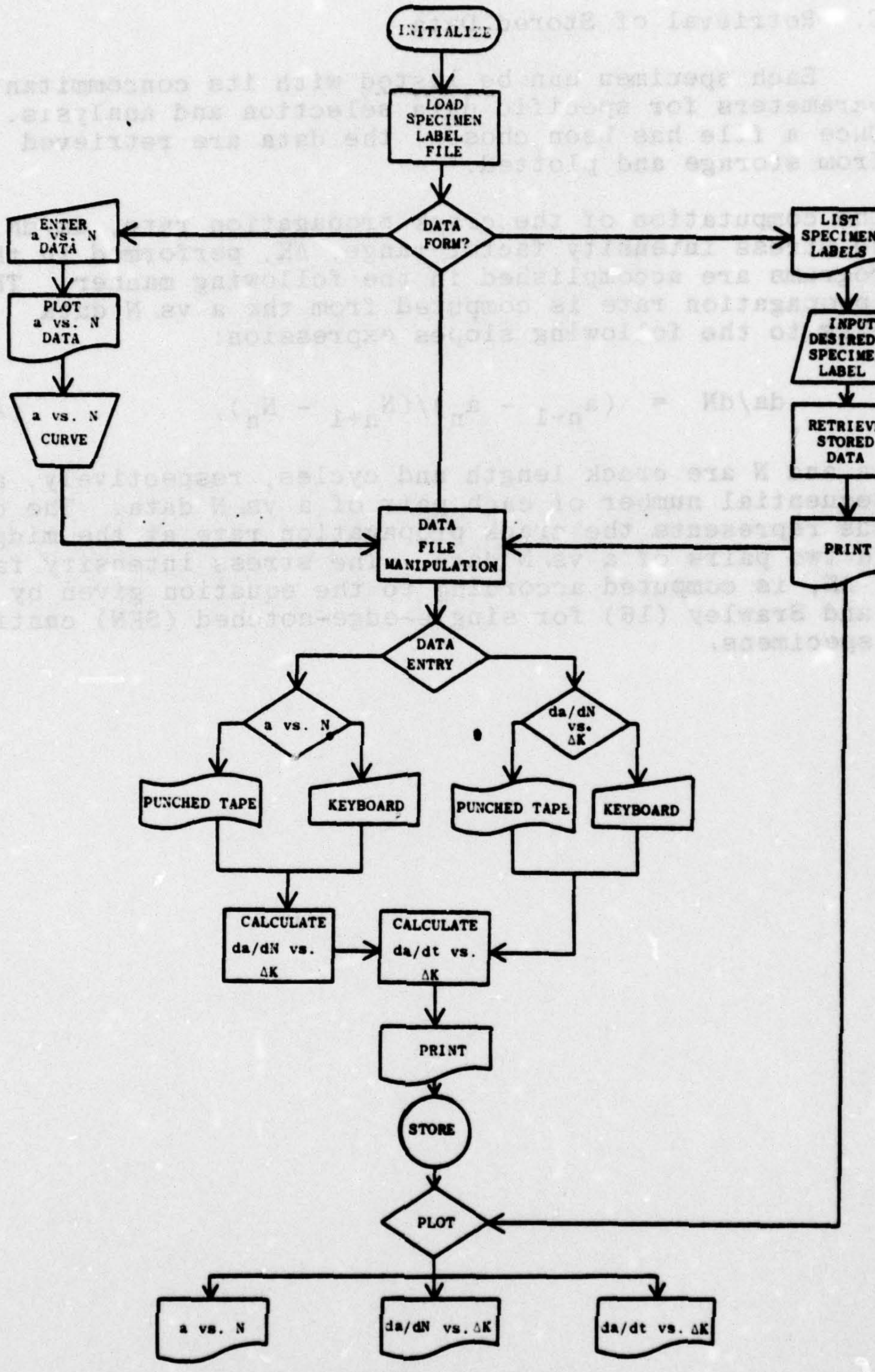

Fig. A-1 - Flow diagram of calculator program for processing, storage, and retrieval of fatigue crack propagation data.